Exploration of Novel TOSMIC Tethered Imidazo[1,2-a]pyridine Compounds for the Development of Potential Antifungal Drug Candidate.

Pratibha Shukla
Guru Gobind Singh Indraprastha University
Deepa Deswal
Guru Gobind Singh Indraprastha University
Mansi Pandit
Sri Venkateswara College
N Latha
Sri Venkateswara College
Divyank Mahajan
University of Delhi - South Campus
Tapasya Srivastava
University of Delhi - South Campus
Anudeep Kumar Narula (aknarula@ipu.ac.in)
GGS Indraprastha University

Research Article

Keywords: Imidazo[1,2-a]pyridine, Multicomponent Reaction, Fluorescence, antioxidant, antifungal, ADME

Posted Date: March 31st, 2021

DOI: https://doi.org/10.21203/rs.3.rs-352624/v1

Abstract

New candidates of imidazo [1, 2-a] pyridine were designed by combining 2-amino pyridine, TOSMIC isocyanide and various assorted aldehydes were synthesized to explore their antioxidant and antifungal potential. The design of these derivatives was based on utilizing the antifungal potential of azoles and TOSMIC moiety. These derivatives were synthesized by adopting multi-component reaction methodology, as it serves as a rapid and efficient tool to target structurally diverse heterocyclic compounds in quantitative yield. The resulting imidazo [1, 2-a] pyridine derivatives were structurally verified by ^{1}HNMR and ^{13}CNMR. The compounds were analyzed for their antioxidant and fluorescent properties and it was observed that compound 15 depicted good fluorescence and antioxidant potential. Additionally, the compounds were evaluated for their antifungal potential against both *Aspergillus fumigatus* 3007 & *Candida albicans* 3018 and it was observed that all the compounds had moderate to significant antifungal effect. Confocal images depicted the porous nature of compound treated fungal cell membranes leading to fungal growth inhibition. Molecular docking was performed to establish the interaction with the target enzyme (Lanosterol 14 alpha demethylase) which also corroborated with the *in vitro* results. *In silico* tools were employed to determine drug-likeliness of the compounds along with determination of ADME properties.

1. Introduction

The importance of heterocyclic compounds is directly associated with the structures that are frequently found in medicines(1). In the family of heterocyclic compounds, the nitrogen atom containing fused bicyclic or tricyclic scaffolds possess very high reactivity(2), which in turn considerably influences their interaction with the biological targets(3). The N-Heterocyclic frameworks are amenable chemical structures used as a “probe” and a “tool” to discover a new lead in medicinal chemistry. Imidazo[1,2-a]pyridines are one of the most widely used N- heterocyclics and have depicted significant biological activity(4) relevant to medicinal applications. Besides their biological application the core also has many applications in electronic devices(5). Additionally, these N- heterocyclic often form a complex π- conjugated system and consequently serve as fluorophores(6). Therefore, owing to their robust applications the development of Nitrogen-rich novel heterocyclic compounds is highly desirable.

The synthesis of imidazo[1,2-a]pyridine structure remains a subject of intense research and efforts have been made to develop new synthetic approaches(7) which includes multicomponent reaction, condensation reaction, oxidative coupling, tandem reaction etc. From this point of view, multicomponent reactions (MCR’s) in combination with post cyclizations is a powerful tool to access complexity and diversity in one step(8-11) to form imidazo [1,2-a] pyridine. In recent decades, there have been numerous classical multicomponent reaction strategies for synthesizing imidazo-fused ring compounds, such as van Leusen imidazole synthesis, Debus-Radziszewski imidazole synthesis, Wallach imidazole synthesis etc(12). Among these synthetic strategies, imidazole synthesis merged with TOSMICs has been recognized as one of the most significant building blocks in N- heterocyclic synthesis. It has also been acknowledged that the combination of any two privileged scaffolds potentially creates more active entities with enhanced biological properties(13). Such types of fused heterocyclic compounds have been reported as important antifungal agents(14). An estimated 1.5- 2.0 million people die of fungal infections each year and approx 1.2 billion individuals are affected by fungal disease each year(15). These emerging threats of fungal infections, direct the synthesis of novel chemical entities with antifungal potential.

Encouraged by these observations and in continuation of our research work to discover novel compounds(16, 17) and by the lead from our previous publication(18), the authors aimed to synthesize TOSMIC fused imidazo [1,2-a] pyridine compounds by using Groebke-Blackburn-Bienayme (GBB) multicomponent reaction. GBB reaction is a three- component- reaction (3CR) to afford the highly complexed structures by using 2-aminopyridine, aldehyde and an isocyanide and proceeds through subsequent formal [4+1] cycloaddition to form highly substituted heterocyclic compounds. Therefore, in the present work the author’s attempt to design an eco- friendly methodology for the synthesis of TOSMIC fused imidazo [1, 2-a] pyridine compounds. All the synthesized analogues were characterized by ^{1}HNMR and ^{13}CNMR. The compounds were additionally evaluated for their antioxidant and fluorescence potential. All the synthesized compounds were tested against both filamentous (*Aspergillusfumigatus* 3007) and unicellular (*Candida albicans* 3018) fungi for their antifungal effect. The potential antifungal compounds were analyzed by HPLC for their purity. Fungal membrane permeablelization was examined by observing the stained mycelia under confocal laser scanning microscope. To further establish the interaction of the compounds with fungal system, *in silico* studies were conducted which depicted interaction of the compounds with amino acid present in the fungal enzyme system. Computational methods predicting drug-likeliness of the compounds were used along with determination of ADME (Absorption, Distribution, Metabolism and Excretion) properties.

2. Results And Discussion

2.1 Chemistry

In the present manuscript, the reaction conditions were optimized using 2-amino pyridine (1, 1mmol), anisaldehyde (2, 1mmol) and TOSMIC (3, 10mmol) as the model substrate for the reaction. The reactants were dissolved in Ethanol and the reaction was allowed to remain on stirring at room temperature in the absence of any catalyst for 10h. The reaction was monitored by TLC and it failed to generate the desired product even after 10h (Table 1, entry 1). Initial effort was to screen the optimal catalyst for the reaction therefore the same set of experiments was then performed with $Sc(OTf)_3$. Reaction was catalyzed with 10 mol% of Sc $(OTf)_3$, it afforded the desired product in 67% of yield (Table 1, entry 2). With the satisfactory result, the reaction was further screened for different catalyst to optimize the reaction conditions, the experimental results are summarized in Table 1 (Entries 3-10). Among the screened catalyst L-Proline was found to be the best for the reaction in terms of yield and reaction time (Table 1, entry 10), this encouraged the authors to use L-Proline as a catalyst for the present reaction. Screening of mol% of catalyst loading is mandatory for the reaction as it affects the yield considerably. When 20 mol% of L- Proline was loaded the yield of the reaction increased significantly (Table 1, entry 11), further increment in the catalyst loading gives

no noteworthy enhancement in yield of the product (Table 1, entry 12). After that the reaction was screened for different solvents. Among the various solvents screened such as non polar (n-Hexane),

Halogenated (DCM), polar aprotic (CH_3CN, THF, CH_3COCH_3, DMF, $CH_3COOC_2H_5$) and polar protic (MeOH, H_2O), a decrease in the yield was observed with the use of non polar and polar aprotic solvents (Table 1, entry 15-19) whereas polar protic gave the product in moderate yield (Table 1, entry 20-22). EtOH was found to be appropriate solvent for the present reaction (Table 1, entry 11). After getting the desired compound in 90% yield by complete conversion of the reactants into products it was established that the reaction medium influenced the process, where L-Proline was used as a catalyst and EtOH as a solvent. Interestingly, the use of L-Proline not only catalyzed the formation of iminium ion but also helps in the transformational diversity(19).

With the optimized conditions in hand, the aldehydic substrate scope on the reaction system was studied (Table 2). The aim of the present work was to reveal the impact of change in aldehydic component on the synthesized compounds. The reaction of 2-amino pyridine (1), assorted aldehydes (2_{1-15}) and TOSMIC (3) were examined; this reaction furnished the corresponding product (Table 2, entry 1-15) in moderate to good yield. The reactivity pattern of different aldehyde is different with other two reactants in terms of yield, but in all cases the electron withdrawing and electron donating substituent (e.g. –CH3, -OCH3, -Cl, -CHO) delivered the product in moderate to good yield (Table 2, entry 2-7) as compared to the non aromatic aldehyde (Table 2, entry 1). The replacement of the phenyl ring by naphthalene moiety had a little impact on the yield of the reaction, inference that the steric properties of the aromatic aldehyde slightly influence the efficacy of the reaction (Table 2, entry 8). Interestingly, in case of naphthalene moiety the reaction proceeds equally well regardless of the substituent (Table 2, entry 9-14). The five member ring tolerated good with the reaction; heteroaryl aldehyde afforded the desired product in excellent yield without affecting the heterocyclic core (Table 2, entry 15). Therefore the present protocol has general applicability with a variety of substituted aldehydes with mild conditions

Based on literature reports(20) and experimental results, the authors proposed a plausible mechanism for the formation of N-(2-(4-methoxyphenyl)imidazo[1,2-a]pyridin-3-yl)-4-methylbenzenesulfonamide (4) in figure (1).

Initially, the mechanism involves the reaction between anisaldehyde [2] and L- Proline leading to the formation of an iminium electrophile which when reacts with the nucleophile (2-amino pyridine [1]) leads to the formation of new bond and the intermediate thus generated releases the L-Proline in its original form. Iminium ion an intermediate [X] further reacts with TOSMIC by formal [4+1] cycloaddition gives nitrilium ion intermediate [Z]. In the last step, nitrilium ion rearomatized followed by a 1, 3- H shift leads to the subsequent ring closure and eventually afforded the desired product.

2.2 Fluorescence Study

According to the literature, imidazo [1, 2-a] pyridine showed an absorption band and an efficient fluorescence band at around 280 and 370 nm respectively(21)**.** It was found during an experimental procedure in the laboratory that these derivatives of imidazo [1, 2-a] pyridine showed blue color under UV- lamp. Consequently, the authors decided to investigate the fluorescence nature of these compounds.

UV characterization for all the compounds was dignified in DMSO and shown in Figure 2(a) (Compound 1-5), Figure 3(a) (Compound 6-10), Figure 4(a) (Compound 11-15). All the compounds displayed 1-3 bands ranging between 200-310 nm this may be attributed to the π-π^* transitions in the complex conjugated system of the compounds. Additionally, most of the derivatives exhibited a broad lower energy band between 350 and 380 nm caused by n-π^* transitions of the non –bonding electrons of the chromophoric group present in the compounds. The emission spectra of all the synthesized compounds were recorded in DMSO at excitation wavelength 280nm at room temperature are shown in Figure 2(b), 3(b) and 4(b) of the compounds 1-5, 6-10 & 11-15 respectively. For each compound the shape of the absorption spectrum agreed with the corresponding excitation spectrum. The fluorescence spectra of the studied compounds exhibited broad band within the range of 354- 461 nm. Among the synthesized compounds 2, 6, 10, 12, 14 & 15 was believed to have efficient fluorescence. Significant changes in the fluorescence are due to the change in the aldehydic component of the compounds. It was observed that the attachment of alkyl aldehyde with imidazo [1, 2-a] pyridine ring has no effect on fluorescence potential (Compound 1) whereas alkyl aldehyde linked with aryl group favors for the enhanced potential (Compound 2). The direct attachment of aryl aldehyde moieties with imidazo [1, 2-a] pyridine sometimes act as a quenchers to suppress fluorescence in some of the molecules regardless of the substituent present on them (Compound 3, 4, 5, 7) (22). Higher fluorescence of Compound 6 than that of the other aryl aldehydes may be explained by the efficient conjugation between the aryl π and the aldehyde (-CHO) π electrons of the compound. The compounds bearing bulkier naphthalene moiety favors for the fluorescence activity in any case of the presence of electron withdrawing or electron donating group(23) (Compound 8, 9, 10, 11, 12 13, 14) but compound 10, 12 & 14 showed remarkable fluorescence as compared to the others, this may be attributed due to the presence of two electron donating methoxy group in Compound 12 adjacent to each other on naphthalene ring. Whereas, the direct attachment of Nitrogen atom with naphthalene influences the conjugation between the lone pair of Nitrogen and π of naphthalene in both Compound 10 & 14 consequently enhances the fluorescence potential. Compound 15 showed remarkable fluorescence emission a broad band around 461 nm, this may be due the presence of five member ring substitution on the imidazo [1, 2-a] pyridine ring, where the Nitrogen atom in five member ring construct the conjugation system between the lone pair and aryl π electrons and thus stabilizes the system for enhance fluorescence.

2.3 Antioxidant activity

Among the synthesized compounds, compound 7, 11, 9, 15 & 13 were believed to be responsible for good antioxidant activity as compared to other synthesized compounds. DPPH inhibitory test was conducted at six different concentrations. The inhibitory effects of synthesized compounds on DPPH are shown by IC_{50} values, calculated and shown in Table 3. Significant change in activity was observed with different functionalities of imidazole cascade. The compound (15) demonstrated the potential antioxidant activity when compared to the reference ascorbic acid because of the presence of

five member ring substitution (pyrrole) adjacent to imidazole ring which stabilizes the unpaired electron and enhances the antioxidant potential of the molecule. Compound (7) having single methoxy on the 4-position of phenyl ring also showed comparable activity with that of reference due to the presence of electron donating methoxy group as reported in literature(24). The lower activity of compound 11 & 9 made us infer that the presence of bulkier naphthalene ring decreases the antioxidant potential of the compounds(25). The authors found that although the compound (13) possesses 2-methoxy group with naphthalene, does not favors for the enhanced activity as this method is selective for the small molecule, and bulkier group shows slow or inert reaction towards antioxidant(26). The other derivatives of aldehyde eventually hamper the antioxidant activity regardless of the substituent present.

2.4 Antifungal potential and Structure-Activity relationship.

All the synthesized compounds were evaluated for their *in vitro* antifungal activity against *Aspergillus fumigates* 3007 and *Candida albicans* 3018. For *A.fumigatus* 3007 the growth inhibiting effect was quantitatively determined by the ratio of diameter of the growth zone in the plate with the synthesized compounds to those with the plate without the compounds (control)(27, 28).

The plates were monitored for 96 hr. While analyzing the antifungal effect, it was observed that all the compounds inhibited the fungal growth but with variable degree (figure 5). Among the synthesized compounds, compound 12 gave the highest inhibitory index of 52.12% after an incubation of 96 hr followed by compounds 15 and 3 with inhibitory index of 49.87 and 43.51% respectively. Compounds 7, 2, 14, 11 and 4 had lowest degree of fungal growth inhibition. However, compounds 1, 6, 9, 10, 13, 8 and 5 had moderate antifungal effect.

Besides filamentous fungus (*A.fumigatus* 3007) the authors also examined the effect of synthesized compounds on unicellular fungus *C.albicans* 3018 after an incubation of 24 hr (Table 4). The compounds were tested in a range of concentration from 0.0976 – 100 µg/ml and it was observed that compound 12 gave the lowest inhibitory concentration of 0.390 µg/ml. Compounds 15 and 3 completely inhibited the fungal growth at a concentration of 0.781 µg/ml. From the observations made it can be concluded that all synthesized compounds had similar inhibitory effect on both filamentous (*A.fumigatus* 3007) and unicellular (*C.albicans* 3018) fungus, thus making them potential candidates with broad spectrum activity for antifungal drug development.

Structure–activity relationship (SAR) studies were carried out to establish a suitable relationship between the functional groups and their effect on antifungal property. Our previous publication and current work clearly suggest that in the formation of imidazo [1, 2-a] pyridine analogues, not only the 2-amino pyridine and isocyanides substitution but the change in nature of substituents on aldehydic component significantly altered the antifungal effect of the synthesized compounds. Results obtained from SAR studies indicated that hydroxyl (-OH) substitution on 2-amino pyridine part, TOSMIC as an isocyanide and either methoxy group on adjacent position of naphthalene or 5-membered ring substitution on aldehydic component, is the paramount combination for the potential antifungal activity. The authors believe that these features of imidazo [1, 2-a] pyridine ring system would further facilitate the applicability of this protocol and the substitutions also lend a hand in the field of medicinal chemistry to form potential antifungal drug candidate.

2.5 Analysis of fungal membrane permeabilization

Cell membrane disruption by inhibition of fungal ergosterol biosynthesis pathway has been documented as the mode of action of azole antifungal agents(29). The cell membrane integrity and porous nature can be determined on the basis of cellular ability to exclude or penetrate dyes by live cells and damaged/necrotic cells(30). In the present study PI dye was used to examine the fungal membrane integrity and thus to generate an insight for a probable antifungal mechanism by the novel synthesized compounds. PI is a plasma membrane impermeable and DNA staining fluorescent probe, which when enters into the cell, intercalates between the DNA bases giving fluorescence(31). In the current work, both treated (grown in the presence of synthesized compound) and control (grown without compound) cells of fungi (*Aspergillusfumigatus* 3007 and *Candida albicans* 3018) were stained with PI dye. Slides were prepared for each section and observed under CLSM (Figure 6 and 7). *A.fumigatus* 3007 cells were grown in the presence of compound 12 for 96 hr and eventually exposed to PI dye. The prepared slides when observed under CLSM depicted fluorescence (Figure 6). The same section under bright field showed fungal mycelia and when the two images (bright field and fluorescent) were superimposed it was apparent that the fluorescence was emitted from within the cells. The untreated fungal mycelium did not display ant detectable red coloured hyphae, thus indicating an uncompromised and intact fungal membrane. Similarly, when *C.albicans* 3018 cells were exposed to compound 12 for 24 hr, it was observed that the cells gave fluorescence upon staining with PI (Figure 7). However, no such fluorescence was observed in control (untreated) samples, which under bright field otherwise showed *C.albicans* 3018 cells.

Parallel observations were notable for both *A.fumigatus* 3007 and *C.albicans* 3018 cells, thus establishing the membrane permeability effect of the synthesized compounds. The test compounds made the plasma membrane porous, thus allowing the PI to enter the cells which resulted in the observed fluorescence. This designates the membrane disruptive nature of the synthesized compounds leading to fungal growth inhibition and the probable mechanism of the compounds.

2.6 Fungal sterol composition

To further strengthen the understanding of the effect of synthesized compounds on the structure of fungal membrane, estimation of fungal sterols in the presence and absence of compounds was carried out. Taking into consideration the multistep sequential synthesis of ergosterol (Fig 8), it is apparent from the figure that inhibition of enzyme lanosterol 14α demethylase would lead to the accumulation of lanosterol and reduction of ergosterol in fungal system. The sterol profile graphs (Figure 9) obtained after the UPLC analysis were consistent with the given hypothesis. In the control sample (without the

compound)-64.91% and 30.78% peak area was reported for lanosterol and ergosterol, respectively. However, when the fungus was grown in the presence of compound 12, there was marked reduction in the peak of ergosterol (7.92%) with an increase in the peak of lanosterol (90.79%), thus highlighting the inhibition of target enzyme (lanosterol 14 α demethylase) by the synthesized compound. The depletion of ergosterol from fungal membrane leads to structural deformities resulting in fungal death.

2.7 *In silico* analysis

Fungi are eukaryotes and share similar cellular and biochemical feature with mammalian cells. Therefore, this necessitates evaluating and examining the present reported compounds for their specificity and selectivity for both fungal and human enzyme system. The synthesized compounds with their imidazole core and hence belong to azole class of antifungal agents. The synthesized compounds have an imidazole core belong to the azole class of antifungal agents. Azoles act by directly inhibiting the synthesis of ergosterol, the primary sterol present in the fungal membrane contributing to membrane fluidity and function(32). Lanosterol 14α-demethylase (CYP51), is the key enzyme that plays a significant role in the ergosterol biosynthesis pathway(29) and therefore was taken as target protein in the present study.

Molecular docking of the in-house library of compounds with CYP51 enzyme from *Aspergillus fumigatus* and *Candida albicans* revealed several promising compounds exhibiting stronger binding with target protein when compared to the existing antifungal fluconazole (Table 5). Among the compounds screened, compound 12 displayed the most significant binding with *Aspergillus* having binding energy value of -58.04 kcal/mol. Observation of the protein-ligand interactions (within 5 Å) showed the presence of several hydrophobic amino acids in the binding pocket with amino acid Asn 398 taking part in hydrogen bond formation and Tyr 122 forming pi-stacking interactions with compound 12 (Figure 10-A). Similarly, a good binding energy value of -51.28 kcal/mol was seen for CYP51-Compound 12 dock complex from *Candida.* Analysis of the binding site showed the presence of both hydrophobic and polar amino acids with His 377 and Tyr 505 forming hydrogen bonds with the compound (Figure 10-B). Further, the interaction of compounds with human counterpart of CYP51 enzyme showed many compounds with comparable binding to the target protein. However, as anticipated compound 12 displayed a lower binding to human CYP51 and is thus expected to preferably bind to fungal enzymes over its human counterpart.

The physicochemical properties of a compound are key determinants of its pharmacokinetic behaviour (ADME; Absorption, Distribution, Metabolism and Excretion). *In silico* prediction of such properties is a critical step in drug discovery process and aids in screening the most promising compounds among many. Our in-house compound library was evaluated for the physicochemical properties using QikProp module from Schrodinger (QikProp, Schrödinger, LLC, New York, NY, 2019). A set of rules known as Lipinski's rule of five(33) evaluates the drug-likeliness of compounds based on molecular structure. All the compounds under study conformed to the rules as they possessed molecular weight less than 500 Da, number of hydrogen bond donors ranged between 1-2 (< 5), number of hydrogen bond acceptors were less than 10 and logP values were between 2 and 5, thus indicating good absorption or penetration. Compounds were stable and not highly flexible in nature since they displayed only 3-6 rotatable bonds (limit: 0-15). Also, polar surface area (PSA) which is Van der Waals surface area of polar nitrogen and oxygen atoms (range: 7-200) and solvent access surface area (SASA) (range: 300-1000) properties which contribute in determination of partition coefficient (logP) and consequently estimate relative hydrophobicity/hydrophylicty of compounds were well-within the specified range. Cumulatively, fewer rotatable bonds and PSA value of less than 140 A2 of all compounds predicted them to exhibit high oral bioavailability(34). Additionally, most compounds manifested great cell permeability in both Caco (human colon adenocarcinoma) and MDCK (Madin-Darby canine kidney cells) permeability models with values more than 500 except compounds 2, 6, 7, 8, 14 and 15 which showed moderate permeability in either model. Furthermore, all compounds displayed high percent human oral absorption (>80%) with most of them predicted to have 100% absorption. Also, the investigated compounds were predicted to have good binding binding to human serum albumin (QPlogKhsa; -1.5-1.5) with compound 4 showing the maximal binding. Overview of physicochemical properties of compound 13 (predicted significant inhibitor compound) revealed it to be a good drug-like candidate with superior oral bioavailability, high percent human oral absorption, cell permeability and human plasma binding (Table 6).

3. Conclusion

Novel N-rich TOSMIC tethered imidazo [1,2-a] pyridine heterocyclic compounds were synthesized via eco-friendly efficient use of Groebke-Blackburn-Bienayme reaction. Among the synthesized compounds, compound 12 & 15 demonstrated most promising fluorescence and antioxidant potential. All the compounds depicted antifungal effect with compound 12 giving the highest antifungal inhibitory index against both *Aspergillus fumigatus* 3007 and *Candidaalbicans* 3018, followed by compound 15. The *in silico* analysis further strengthened the *in vitro* observations as compound 12 interacted with amino acid present in the binding site of target enzyme. Additionally all the compounds abided by the Lipinski's parameters thus, qualifying as potential drug candidate. Therefore, present methodology would serve as a significant tool for generation of relevant antifungal pharmacophore and would find its application in the field of medicinal chemistry.

4. Material And Methods

4.1 Chemistry

All chemicals used in the study were purchased from commercial suppliers. Thin Layer Chromatography (TLC) was performed using Merk F254 aluminum sheets as stationary phase and Ethyl acetate and methanol (70:30) as mobile phase to monitor the reactions. The TLC plate spots were detected by dipping in the Dragendorff's reagent and viewing under UV light. The synthesized compounds were purified using column chromatography. ^{1}HNMR and ^{13}CNMR spectra were obtained using JEOL-400 NMR spectrophotometer at room temperature (RT) using deuterated chloroform ($CDCl_3$) as

solvent and Tetramethylsilane (TMS) as an internal standard. The chemical shifts in NMR spectra are reported as (ppm), coupling constants were reported in Hertz (Hz) and splitting patterns are described as s (singlet), d (doublet), t (triplet), q (quartet), m (multiplet), and dd (doublet of doublet).

4.1.1 Synthesis of the compound 1_{-o}

The title compounds were synthesized as outlined in Figure 11. 2-Aminopyidine (1mmol, 1equiv.), TOSMIC (1mmol, 1equiv.) and the corresponding aldehydes (1mmol, 1equiv.) and L-Proline (20 mol %) were placed in a 50 ml sealed flask equipped with magnetic stirring bar in Ethanol [1mmol= 3ml of ethanol]. Then the mixture was stirred at room temperature (RT) for 6h. Completion of the reaction was observed by TLC using Hexane: Ethyl acetate (1:1) which clearly indicated the disappearance of starting materials and the spot was stained in Dragendorff's reagent which confirmed the formation of new ring system. The solvent was removed by rotary evaporation; complete content was washed with water for the removal of non reacted L- Proline and dried over anhydrous Na_2SO_4 to remove aqueous traces. Finally the product was washed with chloroform: ethanol (8:2) v/v to obtained pure compound. Residue was purified by column chromatography using mixtures of Hexane – EtOAc (v/v) in different proportions to afford the different imidazo[1, 2-a] pyridine derivatives.

4.2. Experimental

The synthesized compounds were characterized by ^{1}HNMR and ^{13}CNMR.

1. **2-isopropyl-N-(tosylmethyl)imidazo[1,2-a]pyridin-3-amine.**

Yield **27%**; ^{1}H NMR (400 MHz, Chloroform-d) δ 8.06 (1 H, s), 7.76 (1 H, d, *J* = 7.8 Hz), 7.37 – 7.28 (1 H, m), 7.27 – 7.10 (1 H, m), 6.90 – 6.42 (1 H, m), 4.69 (2 H, d, *J* = 6.3 Hz), 4.50 – 4.02 (1 H, m), 2.42 (2 H,s), 1.23 (6 H, s).^{13}C NMR (100 MHz, Chloroform -d) δ 160.51, 145.78, 145.35, 133.62, 130.53, 130.13, 129.93, 129.17, 128.95, 128.84, 124.54, 114.16, 109.21, 58.87, 29.78, 22.77, 21.84. LC-MS : *m/z* calculated $[M+H]^+$ = 344.1432, found = 344.1435.

2. **2-phenethyl-N-(tosylmethyl)imidazo[1,2-a]pyridin-3-amine.**

Yield **34%**; ^{1}H NMR (400 MHz, CHLOROFORM-*D*) δ 7.34 – 7.21 (m, 4 H), 7.25 – 7.14 (m, 8 H), 7.14 – 7.05 (m, 1 H), 5.04 – 4.89 (m, 1 H), 3.87 (s, 1 H), 3.59 (d, *J* = 10.9 Hz, 1 H), 3.14 (s, 1H), 3.09 – 2.78 (m, 2 H), 2.75 (d, *J* = 6.0 Hz, 1 H), 2.73 – 2.30 (m, 3H), 2.07 – 1.99 (m, 2 H), 1.42 (d, *J* = 4.9 Hz, 2 H), 1.29 (s, 1 H).13C NMR (100 MHz, Chloroform –d) δ 151.18 145.21, 144.26, 139.24, 138.52, 137.48, 129.94, 128.92, 128.711, 128.47, 128.35, 126.63, 125.21, 117.35, 113.72, 51.95, 25.47, 21.26. LC-MS : *m/z* calculated $[M+H]^+$ = 406.1589, found = 406.1589.

3. **2-(4-butylphenyl)-N-(tosylmethyl)imidazo[1,2-a]pyridin-3-amine.**

Yield **52%**; ^{1}H NMR (400 MHz, Chloroform-*d*) δ 8.01 (1 H, d, *J* = 5.2 Hz), 7.31 (1 H, t, *J* = 7.8 Hz), 7.17 (1 H, d, *J* = 1.4 Hz), 7.07 (2 H, d, *J* = 7.8 Hz), 6.54 – 6.46 (1 H, m), 6.32 – 6.26 (1 H, m), 4.84 (1 H, s), 4.37 (2 H, d, *J* = 5.6 Hz), 2.56 – 2.47 (2 H, m), 1.50 (2 H, q, *J* = 7.7 Hz), 1.36 – 1.22 (2 H, m), 1.18 (1H, s), 0.84 (3 H, td, *J* = 7.3, 1.4 Hz). ^{13}C NMR (100 MHz, Chloroform -*d*) δ 157.91, 157.63, 147.12, 140.96, 136.47, 135.20, 128.03, 127.85, 127.65, 127.26, 126.37, 126.06, 112.02, 105.76, 64.11, 34.76, 34.26, 32.65, 21.33, 12.93. LC-MS : *m/z* calculated $[M+H]^+$ = 434.1902, found = 434.1903.

4. **2-(3,5-di-tert-butylphenyl)-N-(tosylmethyl)imidazo[1,2-a]pyridin-3-amine.**

Yield **57%**; ^{1}H NMR (400 MHz, Chloroform-*d*) δ 8.66 (1 H, dd, *J* = 8.0, 1.2 Hz), 7.87 (1 H, d, *J* = 8.4 Hz), 7.56 – 7.39 (2H, m), 7.36 (1 H, d, *J* = 8.2 Hz), 7.28 – 7.18 (4 H, m), 6.74 (1H, dd, *J* = 6.4, 2.8 Hz), 5.79 – 5.70 (1H, m), 4.97 – 4.82 (2H, m), 2.38 – 2.29 (3H, m), 1.27 (12 H, s), 1.14 (6H, s). ^{13}C NMR (100 MHz, Chloroform -*d*) δ 149.69, 146.02, 144.94, 144.09, 141.93, 135.91, 129.81, 128.97, 128.74, 126.71, 125.18, 125.01, 124.06, 116.35, 114.67, 58.49, 34.68, 31.50, 21.55. LC-MS : *m/z* calculated $[M+H]^+$ = 490.2528, found = 490.2531.

5. **2-(4-chlorophenyl)-N-(tosylmethyl)imidazo[1,2-a]pyridin-3-amine.**

Yield **57%**; ^{1}H NMR (400 MHz, Chloroform-*d*) δ 7.98 – 7.92 (1 H, m), 7.77 (2 H, dt, *J* = 13.9, 5.7 Hz), 7.50 (2 H, d, *J* = 7.9 Hz), 7.41 – 7.09 (1 H, m), 6.58 – 6.44 (2 H, m), 6.08 (1 H, m), 4.92 (1 H, s), 4.22 (2 H, d, *J* = 6.6 Hz), 2.31 (3 H, s).). ^{13}C NMR (100 MHz, Chloroform -*d*) δ 149.87, 145.46, 143.74, 143.18, 136.68, 135.04, 130.46, 129.81, 129.37, 128.87, 128.53, 125.21, 124.81, 116.90, 114.01, 58.92, 21.49. LC-MS : *m/z* calculated $[M+H]^+$ = 412.0886, found = 412.0885.

6. **4-(3-((tosylmethyl)amino)imidazo[1,2-a]pyridin-2-yl)benzaldehyde.**

Yield **70%**; ^{1}H NMR (400 MHz, CHLOROFORM-*D*) δ 9.96 (1 H, s), 8.73 (1 H, d, *J* = 8.2 Hz), 8.42 (2H, d, *J* = 6.9 Hz), 7.81 (1H, d, J = 8.0 Hz), 7.78 – 7.70 (1 H, m), 7.58 (3 H, d, *J* = 9.1 Hz), 7.31 – 7.20 (2H, m), 7.09 (1H, dq, *J* = 13.7, 7.2 Hz), 5.01 (1 H, s), 4.89 (2H, dd, *J* = 25.6, 13.3 Hz), 2.36 (3H, s). ^{13}C NMR (100 MHz, Chloroform-*d*) δ 191.66, 149.49, 145.46, 143.08, 142.57, 137.42, 136.83, 129.76, 129.37, 129.36, 128.92, 127.50, 125.17, 124.91, 116.90, 113.97, 58.92, 21.43. LC-MS : *m/z* calculated $[M+H]^+$ = 406.1225, found = 406.1229.

7. **2-(4-methoxyphenyl)-N-(tosylmethyl)imidazo[1,2-a]pyridin-3-amine.**

Yield **90%**; ^{1}H NMR (400 MHz, Chloroform- d) δ 8.03 – 7.96 (1 H, m), 7.79 – 7.71 (2 H, m), 7.51 – 7.44 (2 H, m), 7.44 – 7.37 (1 H, m), 7.37 – 7.26 (3 H, m), 7.01 – 6.94 (2 H, m), 6.90 (1 H, ddd, *J* = 9.4, 7.2, 1.4 Hz), 4.99 (1 H, d, *J*=14.9 Hz), 5.0 (1 H, s), 4.82 (2 H, d, *J* = 14.9 Hz), 3.85 (3 H, s), 2.43 (3 H, s). ^{13}C NMR (100 MHz, Chloroform-*d*) δ 160.79, 149.49, 145.46, 143.08, 142.82, 136.83, 129.44, 129.21, 128.92, 125.17, 124.91, 124.83, 116.90, 114.06, 113.97, 58.92, 55.36, 21.46. LC-MS : *m/z* calculated $[M+H]^+$ = 408.1382, found = 408.1381.

8. **2-(naphthalen-1-yl)-N-(tosylmethyl)imidazo[1,2-a]pyridin-3-amine.**

Yield **84%**; ^{1}H NMR (400 MHz, Chloroform-*d*) δ 8.07 – 8.00 (1 H, m), 7.99 – 7.91 (2 H, m), 7.84 (1 H, dd, *J* = 9.4, 1.4 Hz), 7.79 – 7.71 (2 H, m), 7.69 – 7.62 (1 H, m), 7.54 (1 H, ddd, *J* = 8.3, 7.0, 1.3 Hz), 7.53 – 7.45 (2 H, m), 7.49 – 7.42 (1 H, m), 7.35 – 7.27 (2 H, m), 7.23 (1 H, ddd, *J* = 9.4, 7.2, 1.3 Hz), 6.90 (1 H, ddd, *J* = 9.4, 7.2, 1.3 Hz), 5.2 (1H, s) 4.99 (2H, d, *J* = 14.9 Hz), 4.82 (1 H, d, *J*=14.9 Hz), 2.42 (3H, s). ^{13}C NMR (100 MHz, Chloroform-*d*) δ 149.69, 145.72, 144.50, 140.69, 136.54, 133.62, 132.55, 129.37, 128.80, 128.30, 127.88, 127.34, 127.23, 127.15, 127.04, 125.59, 125.31, 124.91, 122.22, 117.10, 114.01, 58.92, 21.50. LC-MS : *m/z* calculated $[M+H]^+$ = 428.1432, found = 428.1429.

9. **1-(3-((tosylmethyl)amino)imidazo[1,2-a]pyridin-2-yl)naphthalen-2-ol.**

Yield **84%**; ^{1}H NMR (400 MHz, Chloroform-*d*) δ 9.88 (1 H, d, J = 9.87 Hz) 8.29 (1 H, d, *J* = 8.5 Hz), 8.10 – 7.99 (2 H, m), 7.84 (2 H, d, *J* = 8.5 Hz), 7.69 (5 H, dt, *J* = 27.8, 10.1 Hz), 7.60 – 7.49 (1 H, m), 7.49 – 7.41 (2 H, m), 7.45 – 7.28 (2 H, m), 7.33 – 7.20 (4 H, m), 7.19 (2 H, s), 7.18 – 7.07 (3 H, m), 7.14 (1 H, s), 7.10 – 7.04 (1 H, m), 6.51 (2 H, ddd, *J* = 7.2, 5.4, 1.0 Hz), 6.39 (2 H, dt, *J* = 8.5, 1.0 Hz), 5.21 (1 H, s), 4.83 (2 H, d, *J* = 6.4 Hz), 2.33 (2 H, d, *J* = 17.8 Hz). ^{13}C NMR (100 MHz, Chloroform-d) δ 157.17, 154.80, 145.76, 139.30, 138.24, 136.60, 133.56, 129.80, 129.45, 129.18, 129.02, 127.74, 127.70, 126.66, 125.30, 122.76, 121.53, 121.21, 117.48, 112.95, 110.40, 37.19. LC-MS : *m/z* calculated $[M+H]^+$ = 444.1382, found = 444.1379.

10. **2-(4-(dimethylamino)naphthalen-1-yl)-N-(tosylmethyl)imidazo[1,2-a]pyridin-3-amine.**

Yield **82%**; ^{1}H NMR (400 MHz, Chloroform-*d*) δ 8.14 (1 H, d, *J* = 8.7 Hz), 7.71 (1 H, d, *J* = 8.6 Hz), 7.44 (2 H, d, *J* = 8.0 Hz), 7.34 (1 H, dt, *J* = 23.4, 7.2 Hz), 7.19 (3 H, d, *J* = 3.5 Hz), 7.09 (3 H, d, *J* = 8.2 Hz), 6.87 (1 H, d, *J* = 7.8 Hz), 4.66 (1 H, s), 2.81 (3 H, s), 2.20 (8, d, *J*=80.3 Hz), 1.18 (6H, s). ^{13}C NMR (100 MHz, Chloroform-*d*) δ 149.69, 148.80, 145.72, 144.62, 141.65, 136.27, 131.21, 129.81, 128.98, 128.70, 127.32, 127.19, 127.11, 126.71, 125.76, 125.21, 125.18, 122.46, 116.49, 116.38, 114.33, 58.49, 45.22, 21.51**.** LC-MS : *m/z* calculated $[M+H]^+$ = 471.1854, found = 471.1854.

11. **2-(4-methoxynaphthalen-1-yl)-N-(tosylmethyl)imidazo[1,2-a]pyridin-3-amine.**

Yield **84%**; ^{1}H NMR (400 MHz, Chloroform-*d*) δ 8.05 – 7.98 (1 H, m), 7.94 – 7.87 (1 H, m), 7.91 – 7.81 (2 H, m), 7.78 – 7.70 (2 H, m), 7.56 – 7.47 (2 H, m), 7.42 (1 H, td, *J* = 7.7, 1.2 Hz), 7.33 – 7.23 (3 H, m), 7.04 – 6.97 (1 H, m), 6.92 (1 H, ddd, *J* = 9.3, 7.2, 1.3 Hz), 5.01 (1 H, s) 4.99 (1 H, d, *J* = 15.1 Hz), 4.85 (1 H, d, *J* = 15.1 Hz), 3.84 (3 H, s), 2.44 – 2.39 (3 H, s). ^{13}C NMR (100 MHz, Chloroform-*D*) δ 161.00, 159.14, 156.39, 139.80, 132.07, 132.02, 129.71, 129.67, 126.57, 126.54, 125.70, 125.65, 125.19, 125.15, 125.04, 125.00, 122.54, 122.50, 103.05, 56.16, 56.12, 29.83. LC-MS : *m/z* calculated $[M+H]^+$ = 458.1538, found = 458.1540.

12. **2-(2,3-dimethoxynaphthalen-1-yl)-N-(tosylmethyl)imidazo[1,2-a]pyridin-3-amine.**

Yield **82%**; ^{1}H NMR (400 MHz, Chloroform-*d*) δ 8.00 (1 H, dt, *J* = 6.3, 3.5 Hz), 7.62 (1 H, dt, *J* = 7.0, 3.5 Hz), 7.32 (2 H, dq, *J* = 7.0, 3.6 Hz), 7.19 (2 H, s), 7.08 (1 H, s), 4.91 (1 H, s) 3.88 (6 H, d, *J* = 27.5 Hz), 3.50 (2 H, t, *J* = 6.6 Hz), 2.24 (3 H, m), 1.16 (1 H, s). ^{13}C NMR (100 MHz, Chloroform -*d*) δ 151.85, 150.75,144.42, 143.21, 141.57, 131.56, 130.49, 130.17, 128.94, 128.54, 126.94, 125.93, 125.38, 124.58, 124.36, 120.16, 119.31, 115.03, 113.17, 107.67, 77.43, 63.56, 62.14, 55.71, 29.80. LC-MS : *m/z* calculated $[M+H]^+$ = 488.1644, found = 488.1646.

13. **2-(4,7-dimethoxynaphthalen-1-yl)-N-(tosylmethyl)imidazo[1,2-a]pyridin-3-amine.**

Yield **86%**; ^{1}H NMR (400 MHz, Chloroform-*d*) δ 8.05 – 7.98 (1 H, m), 7.83 – 7.70 (4 H, m), 7.55 – 7.47 (1 H, m), 7.32 – 7.21 (3 H, m), 7.08 – 7.01 (2 H, m), 6.93 (1 H, ddd, *J* = 9.3, 7.2, 1.3 Hz), 6.85 (1 H, dd, *J* = 8.6, 2.0 Hz), 5.12 (1 H, s), 4.99 (1 H, d, *J* = 15.1 Hz), 4.85 (1 H, d, *J* = 15.1 Hz), 3.86 (6 H, s), 2.38 (3 H, m). ^{13}C NMR (100 MHz, Chloroform-*d*) δ 158.65, 152.91, 149.69, 145.72, 143.81, 142.82, 136.27, 129.81, 129.52, 128.74, 126.99, 126.71, 125.61, 125.18, 124.65, 121.20, 116.35, 114.67, 110.21, 106.41, 105.53, 58.49, 56.12, 55.42, 21.54. LC-MS : *m/z* calculated $[M+H]^+$ = 488.1644, found = 4881649.

14. **2-(1-nitronaphthalen-2-yl)-N-(tosylmethyl)imidazo[1,2-a]pyridin-3-amine.**

Yield **82%**; ^{1}H NMR (400 MHz, Chloroform-*d*) δ 8.06 (1 H, dd, *J* = 9.3, 1.5 Hz), 7.97 – 7.87 (2 H, m), 7.84 (1 H, d, *J* = 8.7 Hz), 7.78 – 7.71 (2 H, m), 7.68 (1 H, dd, *J* = 8.8, 0.6 Hz), 7.58 – 7.47 (2 H, m), 7.50 – 7.42 (1 H, m), 7.32 – 7.19 (3 H, m), 6.92 (1 H, ddd, *J* = 9.4, 7.2, 1.3 Hz), 5.02 (1 H, s), 4.99 (1 H, d, *J* = 15.1 Hz), 4.89 (1 H, d, *J* = 14.9 Hz), 2.39 (3 H, s). ^{13}C NMR (100 MHz, Chloroform D) δ 153.71, 153.03, 152.22, 151.02, 148.50, 139.39, 138.54, 135.10, 131.62, 131.07, 130.90, 130.38, 129.91, 128.05, 127.97, 125.63, 125.39, 124.17, 122.35, 121.82, 120.44, 114.22, 29.79. LC-MS : *m/z* calculated $[M+H]^+$ = 473.1283, found = 473.1285.

15. **2-(1H-pyrrol-2-yl)-N-(tosylmethyl)imidazo[1,2-a]pyridin-3-amine.**

Yield **94%**; ^{1}H NMR (400 MHz, Chloroform-*d*) 8.23 (1 H, s), 7.96 – 7.88 (2 H, m), 7.48 (1 H, d, *J* = 2.8 Hz), 7.34 – 7.23 (2 H, m), 7.00 (`1 H, dd, *J* = 4.0, 2.8 Hz), 6.80 (1 H, dd, *J* = 3.8, 1.2 Hz), 4.91 (1 H, s), 2.39 (3 H, s), 1.23 (2 H, s). ^{13}C NMR (100 MHz, Chloroform -*d*) δ 148.59, 144.55, 141.16, 138.80, 136.59, 129.82, 128.69, 127.95, 123.76, 118.58, 115.44, 113.96, 106.28, 62.82, 21.74. LC-MS : *m/z* calculated $[M+H]^+$ = 367.1228, found = 367.1235.

4.3 Fluorescence study.

At 25^{0}C, the UV-vis absorbance was measured within the range 200-450 nm for all the derivatives using a 3-5 nm quartz cuvette on a Hitachi U-2900 spectrophotometer. The Fluorescence spectra of each compound were obtained in DMSO solution at 25^{0}C on a Varian Cary Eclipse Fluorescence Spectrophotometer

4.4 Analysis of antioxidant activity

Determination of DPPH radical –scavenging activity:

The radical inhibition action of the synthesized compounds was accessed by DPPH assay method. The DPPH method was selective for the antioxidant activity because it is the most effective method for calculating radical scavenging capacity by a chain-breaking mechanism(35). As indicated by the methodology, 3ml of 0.004 % DPPH was mixed with 1ml of (1-500 µg/ml) standard or synthesized compounds. The standard used for activity is ascorbic acid. The solutions were well mixed and the reaction was incubated in dark for 30min at RT. Furthermore, the absorption activity was analyzed spectrophotometrically at 517nm. The absorbance value of DPPH in methanol alone was presented as absorbance of blank. The absorbance value of compounds and standard when mixed with DPPH in methanol was presented as absorbance of sample and standard respectively.

The percentage radical scavenging activity was computed by the formula:

$$\% \text{ radical scavenging activity} = \frac{\text{(Absorbance of blank – absorbance of sample or standard) after 30min}}{\text{(Absorbance of Blank) after 30 min}} * 100$$

IC_{50} was measured from graphical method by plotting percentage inhibition Vs concentration for both sample and standard.

4.5 Antifungal activity

4.5.1 Material

The media components were procured from Hi-Media Laboratory Pvt. Ltd. (Mumbai, India); RPMI and MOPS (3-[N-morpholino]propanesulfonic acid) from Sigma-Aldrich Chemical Co. (St. Louis, USA).

4.5.2 Microorganism and culture conditions

Aspergillus fumigatus 3007 and *Candida albicans* 3018 were procured from Microbial type culture collection (MTCC), Chandigarh, India. *A.fumigatus* 3007 was grown and maintained on malt extract agar (MEA) composed of (g/l): malt extract, 20.0; and agar, 20.0 at 30°C. *C.albicans* 3018 was grown and maintained on (g/l): malt extract, 3.0; yeast extract, 3.0; peptone, 5.0; glucose, 10.0; and agar, 20.0 at 35°C. The fungal cultures were maintained by periodical sub culturing and stored at 4°C.

4.5.3 Antifungal activity

The antifungal inhibitory assay was performed by the plate growth rate method for *A.fumigatus* 3007. The synthesized compounds and fluconazole were dissolved in 1% DMSO at a concentration of 5 mg/ml. Each solution was then added individually to 20ml of sterile MEA to give a final concentration of 0.1mg/ml. The solutions were poured into sterile petri dishes. Control plates were prepared without the compounds. A mycelia disk (8mm dia) was cut from the advancing margins of growing fungal cultures and seeded into the centre of each plate and incubated at 30°C for different time intervals. The radial colony growth was measured daily until the fastest growing colony (control) had reached the edge of the plate. The antifungal inhibitory index was calculated using the following equation:

$$\text{Antifungal inhibitory index (\%)} = [(D_b - D_a)/D_b] \text{ X } 100$$

Where 'D_b' is colony diameter in control and 'D_a' is colony diameter in the test plates.

The minimum inhibitory concentration values for all the derivatives against *C.albicans* 3018 were determined by microdilution method in 96 well microtiter plates as described in the Clinical and Laboratory Standard Institute (CLSI) document M27-A3 with minor modifications. A single colony from 24 h old culture of *C.albicans* 3018 was used to inoculate 5 ml of Potato Dextrose Broth medium and incubated overnight with shaking at 35°C. 100µl of actively growing yeast culture was then transferred to 900 µl of double distilled water and readjusted to achieve OD_{600} of 0.12 (~1x10^6 cfu/ml). The cell

suspension was further diluted to achieve $1x10^3$ – $5x10^3$ cfu/ml in RPMI1640 medium [RPMI medium was made as per the CLSI guidelines and was buffered to pH 7.0 with 0.165M MOPS buffer]. Two fold serial dilutions of all the synthesized compounds and fluconazole was prepared in 96 well microplates with RPMI1640 growth media (100µl) to achieve final concentration from 0.0976-100 µg/ml. 100µl of cell suspension was added to each well which provided the final inoculum size of $0.5x10^3$ cfu/ml.

4.5.4 Ultra structure analysis of fungal membrane

Experimental mycelia (*A.fumigatus* 3007) of treated fungal sample was collected after 96 h of incubation period and slides were prepared as reported earlier(36)

C.albicans 3018 cells were taken at a concentration of $0.5x10^3$ cfu/ml in RPMI1640 growth medium and grown overnight at 35°C at 200 rpm in the presence of compound 12 at concentration of 0.781 µg/ml for 24 h. Subsequently, cells were treated with Propidium iodide (PI, 20µM) for 10 minutes at room temperature. Glass slides were prepared for all the samples and observed using Leica TCS SP5 confocal scanning microscope.

4.5.5 Determination of fungal sterol composition

Erlenmeyer flask (250 ml) containing 50 ml of 2% malt extract broth (HiMedia) was autoclaved and at room temperature compound 12 was added to the flask to give a final concentration of 0.1 mg/ml under sterile conditions. The flask without the compound was taken as control. Each flask was inoculated with four fungal mycelia discs (8 mm diameter each) cut from the growing margins of *Aspergillus fumigates* 3007 and incubated at 30°C for 6 days. The fungal mat thus formed was harvested from the flask and homogenized with a pestle and mortar for ergosterol extraction as reported earlier(18).

The fractions were analysed using UPLC (Waters), with the mobile phase a mixture of 95% methanol:acetonitrile (1:1) with 5% water, and the column used was C18. The flow rate of mobile phase was 0.4 ml/min and the column temperature was 30°C. The ergosterol peak eluted at 4.883 minute, while the lanosterol peak eluted at 0.697 minute.

4.6 *In silico* receptor binding study

To obtain more insights into enzyme-inhibitor interactions, molecular docking study was carried out. Protein-ligand docking was performed for all 15 compounds with CYP51 enzyme from *Aspergillus fumigatus* (PDB ID: 6CR2)(37) *Candida albicans* (PDB ID: 5V5Z)(38) and *Homo sapiens* (PDB ID: 3LD6)(39)**.** The 2D chemical structures of compounds were drawn via Marvin Sketch (version 15.4.20.0) and their physicochemical properties were calculated using QikProp. Prior to molecular docking, ligand structures were prepared using LigPrep module(40). The structures of target proteins were prepared using Protein Preparation wizard (Schrodinger, LLC, New York, NY, 2019) which involved addition of hydrogen atoms, assigning of bond orders, formation of disulphide bonds and removal of heteroatoms while retaining heme co-factor followed by energy minimization and refinement. Subsequently, molecular docking was done using Extra- Precision (XP) mode of Glide(41) where ligand molecules were docked into the binding site defined by the co-crystallised (inhibitor) molecule. A binding free energy (ΔG bind) for each docked pose was further estimated using Prime MM-GBSA method ENREF_26 (42).

Declarations

Acknowledgement

The PS, DD and AKN are grateful to Guru Gobind Singh Indraprastha University (GGSIPU), New Delhi, India, for the financial support during the progress of the present work. PS would also like to thank Mr. Naveen for the analytical support of NMR data and Dr. Preeti Sehgal for critically evaluating the manuscript. DD would like to thank Dr.Charu from Central Instrumentation Facility, University of Delhi South Campus for confocal images.

Conflict of interest: The authors have no conflict of interest.

References

1. Balwe S, Jeong Y. An approach towards the synthesis of novel fused nitrogen tricyclic heterocyclic scaffolds via GBB reaction. Organic & biomolecular chemistry. 2018;16 8:1287-96.
2. Flick AC, Ding HX, Leverett CA, Kyne RE, Jr., Liu KK, Fink SJ, et al. Synthetic Approaches to the New Drugs Approved During 2015. Journal of medicinal chemistry. 2017 Aug 10;60(15):6480-515. PubMed PMID: 28421763. Epub 2017/04/20. eng.
3. Jordan AM, Roughley SD. Drug discovery chemistry: a primer for the non-specialist. Drug discovery today. 2009 Aug;14(15-16):731-44. PubMed PMID: 19416759. Epub 2009/05/07. eng.
4. Tan H, Wang Y. Facile Synthesis of Novel Hexahydroimidazo[1,2-a]pyridine Derivatives by One-Pot, Multicomponent Reaction under Ambient Conditions. ACS Combinatorial Science. 2020 2020/07/07.
5. Chen WC, Yuan Y, Xiong Y, Rogach AL, Tong QX, Lee CS. Aromatically C6- and C9-Substituted Phenanthro[9,10-d]imidazole Blue Fluorophores: Structure-Property Relationship and Electroluminescent Application. ACS applied materials & interfaces. 2017 Aug 9;9(31):26268-78. PubMed PMID: 28692277. Epub 2017/07/12. eng.

6. Benson N, Suleiman O, Odoh SO, Woydziak ZR. Pyrazole, Imidazole, and Isoindolone Dipyrrinone Analogues: pH-Dependent Fluorophores That Red-Shift Emission Frequencies in a Basic Solution. The Journal of organic chemistry. 2019 Sep 20;84(18):11856-62. PubMed PMID: 31438666. Pubmed Central PMCID: PMC7082152. Epub 2019/08/24. eng.
7. Devi N, Singh D, Rawal RK, Bariwal J, Singh V. Medicinal Attributes of Imidazo[1,2-a]pyridine Derivatives: An Update. Current topics in medicinal chemistry. 2016;16(26):2963-94. PubMed PMID: 27150367. Epub 2016/05/07. eng.
8. Rotstein BH, Zaretsky S, Rai V, Yudin AK. Small heterocycles in multicomponent reactions. Chemical reviews. 2014 Aug 27;114(16):8323-59. PubMed PMID: 25032909. Epub 2014/07/18. eng.
9. Neochoritis CG, Zhao T, Dömling A. Tetrazoles via Multicomponent Reactions. Chemical reviews. 2019;119(3):1970-2042. PubMed PMID: 30707567. Epub 02/01. eng.
10. Ahmadi T, Mohammadi Ziarani G, Gholamzadeh P, Mollabagher H. Recent advances in asymmetric multicomponent reactions (AMCRs). Tetrahedron: Asymmetry. 2017 2017/05/15/;28(5):708-24.
11. Kumar RS, Rajesh SM, Perumal S, Banerjee D, Yogeeswari P, Sriram D. Novel three-component domino reactions of ketones, isatin and amino acids: Synthesis and discovery of antimycobacterial activity of highly functionalised novel dispiropyrrolidines. Eur J Med Chem. 2010 2010/01/01/;45(1):411-22.
12. Zheng X, Ma Z, Zhang D. Synthesis of Imidazole-Based Medicinal Molecules Utilizing the van Leusen Imidazole Synthesis. Pharmaceuticals (Basel). 2020;13(3):37. PubMed PMID: 32138202. eng.
13. Ji H, Stanton BZ, Igarashi J, Li H, Martásek P, Roman LJ, et al. Minimal Pharmacophoric Elements and Fragment Hopping, an Approach Directed at Molecular Diversity and Isozyme Selectivity. Design of Selective Neuronal Nitric Oxide Synthase Inhibitors. Journal of the American Chemical Society. 2008 2008/03/01;130(12):3900-14.
14. Fuentefria AM, Pippi B, Dalla Lana DF, Donato KK, de Andrade SF. Antifungals discovery: an insight into new strategies to combat antifungal resistance. Letters in applied microbiology. 2018 Jan;66(1):2-13. PubMed PMID: 29112282. Epub 2017/11/08. eng.
15. Flevari A, Theodorakopoulou M, Velegraki A, Armaganidis A, Dimopoulos G. Treatment of invasive candidiasis in the elderly: a review. Clin Interv Aging. 2013;8:1199-208. PubMed PMID: 24043935. Epub 09/09. eng.
16. Azad CS, Saxena AK. Stereoconvergent synthesis of 1-deoxynojirimycin isomers by using the 3 component 4 centred Ugi reaction. Organic Chemistry Frontiers. 2015;2(6):665-9.
17. Azad CS, Khan IA, Narula AK. Organocatalyzed asymmetric Michael addition by an efficient bifunctional carbohydrate–thiourea hybrid with mechanistic DFT analysis. Organic & Biomolecular Chemistry. 2016;14(48):11454-61.
18. Shukla P, Deswal D, Azad CS, Narula AK. Novel nucleosides as potential inhibitors of fungal lanosterol 14α-demethylase: an in vitro and in silico study. Future medicinal chemistry. 2019 Oct;11(20):2663-86. PubMed PMID: 31637926. Epub 2019/10/23. eng.
19. Balwe SG, Jeong YT. An approach towards the synthesis of novel fused nitrogen tricyclic heterocyclic scaffolds via GBB reaction. Organic & Biomolecular Chemistry. 2018;16(8):1287-96.
20. Dömling A, Wang W, Wang K. Chemistry and biology of multicomponent reactions. Chemical reviews. 2012 Jun 13;112(6):3083-135. PubMed PMID: 22435608. Pubmed Central PMCID: PMC3712876. Epub 2012/03/23. eng.
21. Stasyuk AJ, Banasiewicz M, Cyrański MK, Gryko DT. Imidazo[1,2-a]pyridines Susceptible to Excited State Intramolecular Proton Transfer: One-Pot Synthesis via an Ortoleva–King Reaction. The Journal of organic chemistry. 2012 2012/07/06;77(13):5552-8.
22. Guo H-M, Tanaka F. A fluorogenic aldehyde bearing a 1,2,3-triazole moiety for monitoring the progress of aldol reactions. The Journal of organic chemistry. 2009;74(6):2417-24. PubMed PMID: 19222210. eng.
23. Yee DJ, Balsanek V, Sames D. New Tools for Molecular Imaging of Redox Metabolism: Development of a Fluorogenic Probe for 3α-Hydroxysteroid Dehydrogenases. Journal of the American Chemical Society. 2004 2004/03/03;126(8):2282-3.
24. Naik N. Three component one pot synthesis of 5-Substituted 1-Aryl-2,3-diphenyl imidazoles: A novel class of promising antioxidants. Journal of Applied Pharmaceutical Science. 2012 11/29.
25. Hasan HA, Abdulmalek E, Saleh TA, Abdul Rahman MB, Shaari KB, Yamin BM, et al. Synthesis of novel 6-substituted-5,6-Dihydrobenzo[4,5] Imidazo[1,2-c] quinazoline compounds and evaluation of their properties. Journal of Molecular Structure. 2019 2019/10/05/;1193:482-94.
26. Lloyd WG, Zimmerman RG, Dietzler AJ. Antioxidant Inhibition by Substituted Phenols. Antioxidant Efficacy as a Function of Structure and Reactivity. I&EC Product Research and Development. 1966 1966/12/01;5(4):326-30.
27. Deswal D, Shukla P, Azad CS, Narula AK. Carbohydrate hitched imidazoles as agents for the disruption of fungal cell membrane. Journal de mycologie medicale. 2020 Apr;30(1):100910. PubMed PMID: 31806380. Epub 2019/12/07. eng.
28. Nainwal L, Azad DC, Deswal D, Narula A. Exploration of Antifungal Potential of Carbohydrate-Tethered Triazoles as CYP450 Inhibitors. ChemistrySelect. 2018 10/17;3:10762-7.
29. Geißel B, Loiko V, Klugherz I, Zhu Z, Wagener N, Kurzai O, et al. Azole-induced cell wall carbohydrate patches kill Aspergillus fumigatus. Nature Communications. 2018 12/01;9.
30. Dananjaya SHS, Udayangani RMC, Shin SY, Edussuriya M, Nikapitiya C, Lee J, et al. In vitro and in vivo antifungal efficacy of plant based lawsone against Fusarium oxysporum species complex. Microbiological research. 2017 Aug;201:21-9. PubMed PMID: 28602398. Epub 2017/06/13. eng.

31. Fosso MY, Shrestha SK, Green KD, Garneau-Tsodikova S. Synthesis and Bioactivities of Kanamycin B-Derived Cationic Amphiphiles. Journal of medicinal chemistry. 2015 Dec 10;58(23):9124-32. PubMed PMID: 26592740. Pubmed Central PMCID: PMC5154386. Epub 2015/11/26. eng.
32. Lass-Flörl C. Triazole Antifungal Agents in Invasive Fungal Infections. Drugs. 2011 2011/12/01;71(18):2405-19.
33. Lipinski CA, Lombardo F, Dominy BW, Feeney PJ. Experimental and computational approaches to estimate solubility and permeability in drug discovery and development settings. Adv Drug Deliv Rev. 2001 Mar 1;46(1-3):3-26. PubMed PMID: 11259830. Epub 2001/03/22. eng.
34. Veber DF, Johnson SR, Cheng HY, Smith BR, Ward KW, Kopple KD. Molecular properties that influence the oral bioavailability of drug candidates. Journal of medicinal chemistry. 2002 Jun 6;45(12):2615-23. PubMed PMID: 12036371. Epub 2002/05/31. eng.
35. Abdel-Wahab BF, Awad GE, Badria FA. Synthesis, antimicrobial, antioxidant, anti-hemolytic and cytotoxic evaluation of new imidazole-based heterocycles. Eur J Med Chem. 2011 May;46(5):1505-11. PubMed PMID: 21353349. Epub 2011/03/01. eng.
36. Deswal D, Shukla P, Azad DC, Narula A. Carbohydrate hitched imidazoles as agents for the disruption of fungal cell membrane. Journal de mycologie medicale. 2019 11/01;30:100910.
37. Friggeri L, Hargrove TY, Wawrzak Z, Blobaum AL, Rachakonda G, Lindsley CW, et al. Sterol 14α-Demethylase Structure-Based Design of VNI ((R)- N-(1-(2,4-Dichlorophenyl)-2-(1 H-imidazol-1-yl)ethyl)-4-(5-phenyl-1,3,4-oxadiazol-2-yl)benzamide)) Derivatives To Target Fungal Infections: Synthesis, Biological Evaluation, and Crystallographic Analysis. Journal of medicinal chemistry. 2018 Jul 12;61(13):5679-91. PubMed PMID: 29894182. Pubmed Central PMCID: PMC6176729. Epub 2018/06/13. eng.
38. Keniya MV, Sabherwal M, Wilson RK, Woods MA, Sagatova AA, Tyndall JDA, et al. Crystal Structures of Full-Length Lanosterol 14α-Demethylases of Prominent Fungal Pathogens Candida albicans and Candida glabrata Provide Tools for Antifungal Discovery. Antimicrob Agents Chemother. 2018;62(11):e01134-18. PubMed PMID: 30126961. eng.
39. Strushkevich N, Usanov S, Park H-w. Structural Basis of Human CYP51 Inhibition by Antifungal Azoles. Journal of molecular biology. 2010 02/01;397:1067-78.
40. Sastry GM, Adzhigirey M, Day T, Annabhimoju R, Sherman W. Protein and ligand preparation: parameters, protocols, and influence on virtual screening enrichments. Journal of computer-aided molecular design. 2013 Mar;27(3):221-34. PubMed PMID: 23579614. Epub 2013/04/13. eng.
41. Friesner RA, Murphy RB, Repasky MP, Frye LL, Greenwood JR, Halgren TA, et al. Extra precision glide: docking and scoring incorporating a model of hydrophobic enclosure for protein-ligand complexes. Journal of medicinal chemistry. 2006 Oct 19;49(21):6177-96. PubMed PMID: 17034125. Epub 2006/10/13. eng.
42. Rastelli G, Del Rio A, Degliesposti G, Sgobba M. Fast and accurate predictions of binding free energies using MM-PBSA and MM-GBSA. Journal of computational chemistry. 2010 Mar;31(4):797-810. PubMed PMID: 19569205. Epub 2009/07/02. eng.

Tables

Table 1: Optimization of the reaction conditions

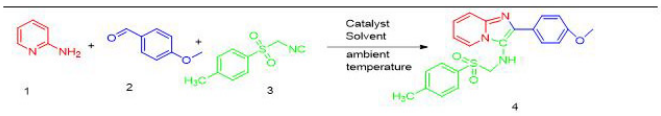

Entry	Catalyst (mol %)	Solvent	Time[h]	% Yield
1	-	EtOH	10	-
2	$Sc(OT)_3$ (10)	EtOH	10	67
3	I_2 (10)	EtOH	10	56
4	H_3BO_3 (10)	EtOH	10	54
5	ZnO (10)	EtOH	10	62
6	TBHP (10)	EtOH	10	67
7	TBBA (10	EtOH	10	62
8	$ZnCl_2$ (10)	EtOH	10	43
9	$FeCl_3$ (10)	EtOH	10	40
10	L-Proline (10)	EtOH	6	88
11	L-Proline (20)	EtOH	4	90
12	L-Proline (40)	EtOH	4	89
13	L-Proline (20)	n-Hexane	4	60
14	L-Proline (20)	DCM	4	72
15	L-Proline (20)	CH_3CN	4	78
16	L-Proline (20)	THF	4	78
17	L-Proline (20)	Acetone	4	67
18	L-Proline (20)	DMF	4	70
19	L-Proline (20)	Ethyl Acetate	4	72
20	L-Proline (20)	n-Butanol	4	82
21	L-Proline (20)	CH_3OH	4	86
22	L-Proline (20)	H2O	4	84

[a]Reaction conditions: Reaction was carried out using 1 (1mmol), 2 (1mmol), 3 (1mmol), catalyst 10 or 20mol%, in solvent (3 mL) at RT [b]Isolated yields after column chromatography.

Table 2: Substrate scope

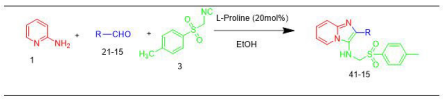

Entry	$R_{1\text{-}15}$	Time	% Yield
1		6h	27
2		6h	34
3		6h	52
4		6h	57
5		6h	57
6		8	70
7		8	90
8		8	84
9		8	84
10		8	82
11		8	84
12		8	82
13		8	86
14		8	82
15		8	94

[a]Reaction conditions: Reaction was carried out using 1 (1mmol), $2_{1\text{-}15}$ (1mmol), 3 (1mmol), catalyst 20mol%, in EtOH (3 mL) at RT , [b]Isolated yields after column chromatography

Table 3: IC_{50} values of the compounds

COMPOUND	R	DPPH IC_{50} (µg/ml) ±SD
1	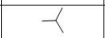	105.2 ± 2.00
2	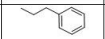	57.9 ± 0.44
3	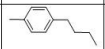	63.2 ± 1.32
4	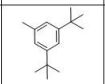	67.5 ± 0.85
5		123 ± 1.92
6	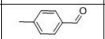	51.6 ± 0.44
7	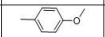	26.45 ± 0.66
8	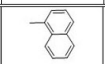	54.6 ± 0.26
9	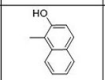	49.6 ± 0.48
10	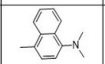	68.9 ± 0.62
11	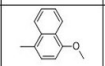	48.9 ± 0.45
12	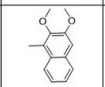	97.6 ± 0.71
13	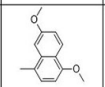	47.6 ± 0.63
14	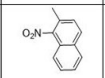	67.9 ± 1.24
15	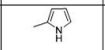	22.45 ± 1.82
16	Ascorbic Acid	21.8 ± 1.23

Table 4: Minimum Inhibitory Concentration for *Candida albicans* 3018 after 24 hr

Compound	Minimum Inhibitory Concentration (µg/ml)
1	>100
2	>50
3	0.781
4	>50
5	>100
6	>50
7	>50
8	>100
9	>50
10	>50
11	>100
12	0.390
13	>50
14	>50
15	0.781
Flu	0.097

Table 5: Binding free energy (ΔG) values for dock complexes of compounds with CYP51 from *Aspergillus fumigatus*, *Candida albicans* and *Homo sapiens*

Compound	Binding free energy (ΔG)		
	Aspergillus fumigatus	*Candida albicans*	*Homo sapiens*
1	-28.80	-25.25	-34.58
2	-37.38	-1.71	-15.86
3	-53.28	-11.32	-44.77
4	-1.90	-51.94	-48.01
5	-28.77	-27.47	-44.13
6	-22.00	No good pose	-55.53
7	-37.78	-10.60	-51.40
8	-6.53	-19.15	-46.08
9	No good pose	-17.53	-52.12
10	-17.51	-48.08	-37.57
11	-36.56	-38.27	-52.24
12	-58.04	-51.28	-41.14
13	-43.84	-56.34	-40.15
14	-26.49	No good pose	-48.98
15	No good pose	-15.19	-39.50
Fluconazole	-18.34	-22.55	-28.99

Table 6: Physicochemical properties of compounds

Compound	RB	MW (Da)	D-HB	A-HB	logP	PSA	SASA	Metab	PercentHumanOral Absorption	QPP Caco	QPP MDCK	QPlogKhsa
1	4	329.416	1	6	3.264	61.148	610.302	2	100	2592.168	1,404.818	0.17
2	6	391.487	1	6	4.472	59.863	656.198	3	100	2690.483	431.994	0.482
3	6	419.54	1	6	5.047	61.172	739.761	2	100	1524.94	718.415	0.829
4	5	475.648	1	6	5.952	59.69	745.056	3	100	1659.912	788.28	1.305
5	3	397.878	1	6	4.698	60.191	712.218	1	100	1540.074	700.112	0.634
6	4	391.444	1	8	3.007	97.435	686.864	1	100	285.721	699.763	0.198
7	4	393.459	1	6.75	4.257	68.533	709.632	2	95.449	1538.828	396.769	0.514
8	3	413.493	1	6	4.091	60.92	623.021	1	88.507	1366.867	127.729	0.533
9	4	429.492	2	6.75	3.618	79.07	621.389	2	100	873.366	1,948.23	0.403
10	4	456.561	1	7	4.328	64.423	657.19	2	100	1362.166	1,441.935	0.608
11	4	443.519	1	6.75	4.145	68.062	639.775	2	100	1394.782	855.531	0.52
12	5	473.545	1	7.5	4.747	72.255	712.057	3	100	1996.755	1,044.638	0.651
13	5	473.545	1	7.5	4.259	75.993	668.735	3	100	1704.307	890.043	0.499
14	4	458.491	1	7	3.998	103.298	699.752	2	100	347.338	780.593	0.604
15	3	352.41	2	6	2.8	74.4	559.489	1	100	815.375	95.832	0.167
RB- Number of non-trivial (not CX3), non-hindered (not alkene, amide, small ring) rotatable bonds.												
MW- Molecular weight of the molecule.												
SASA- Total solvent accessible surface area (SASA) in square angstroms using a probe with a 1.4 Å radius.												
D-HB Estimated number of hydrogen bonds that would be donated by the solute to water molecules in an aqueous solution. Values are averages taken over a number of configurations, so they can be non-integer.												
A-HB Estimated number of hydrogen bonds that would be accepted by the solute from water molecules in an aqueous solution. Values are averages taken over a number of configurations, so they can be non-integer.												
logP- Predicted octanol/water partition coefficient.												
PSA- Van der Waals surface area of polar nitrogen and oxygen atoms.												
Percent HumanOralAbsorption- Predicted human oral absorption on 0 to 100% scale.The prediction is based on a quantitative multiple linear regression model. This property usually correlates well with HumanOralAbsorption, as both measure the same property												
Metab -umber of likely metabolic reactions												
QPPCaco- Predicted apparent Caco-2 cell permeability in nm/sec. Caco2 cells are a model for the gut-blood barrier.												
QPPMDCK- Predicted apparent MDCK cell permeability in nm/sec. MDCK cells are considered to be a good mimic for the blood-brain barrier.												
QPlogKhsa- Prediction of binding to human serum albumin												

Figures

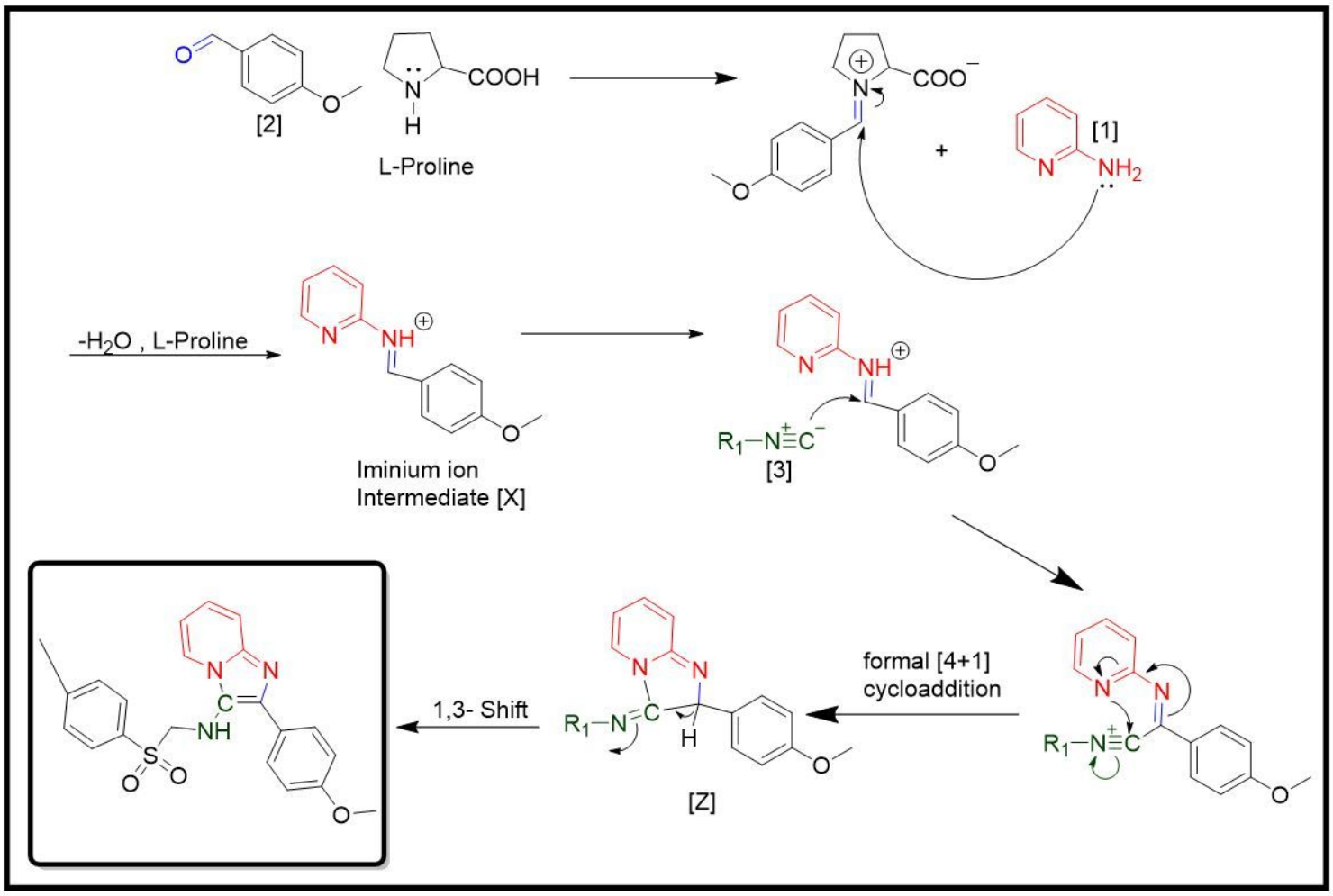

Figure 1

Plausible Reaction Mechanism

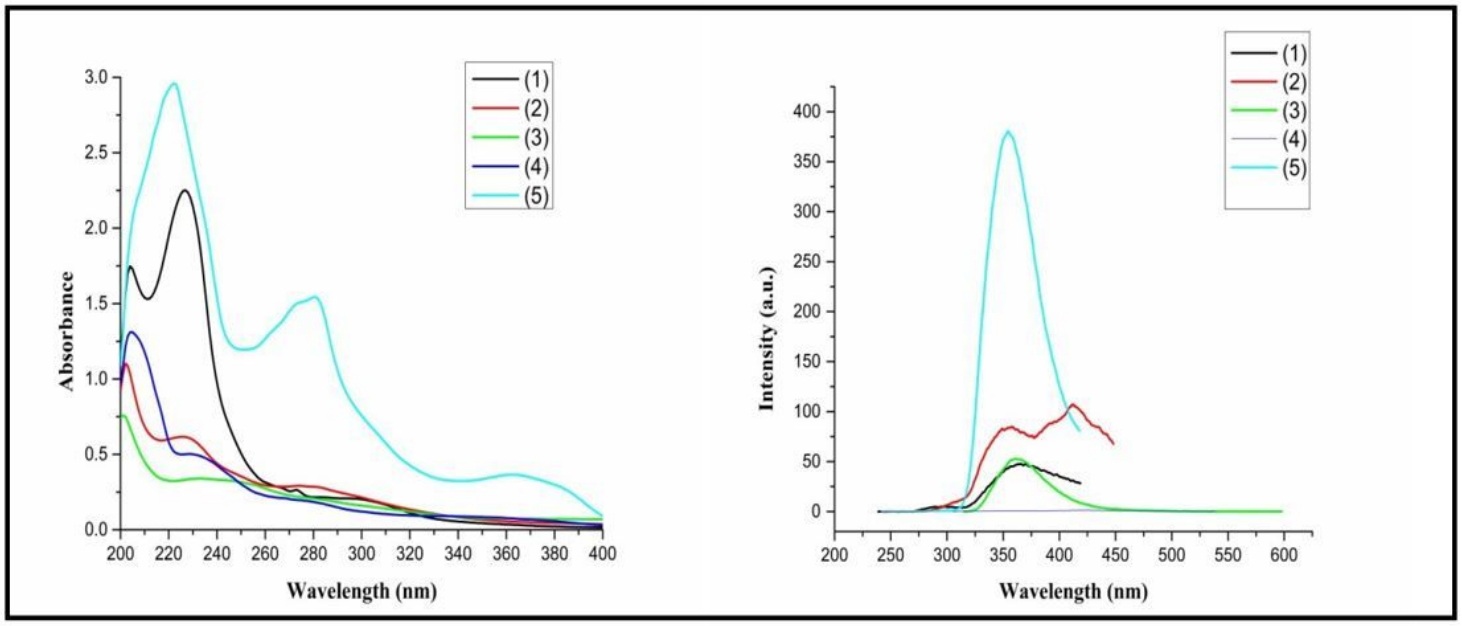

Figure 2

(a): UV-vis absorption spectra of compound (1-5) DMSO solution. (b):Fluorescence emission vspectra of the compound in (1-5) at excitation wavelength of 280 nm in DMSO solution at RT.

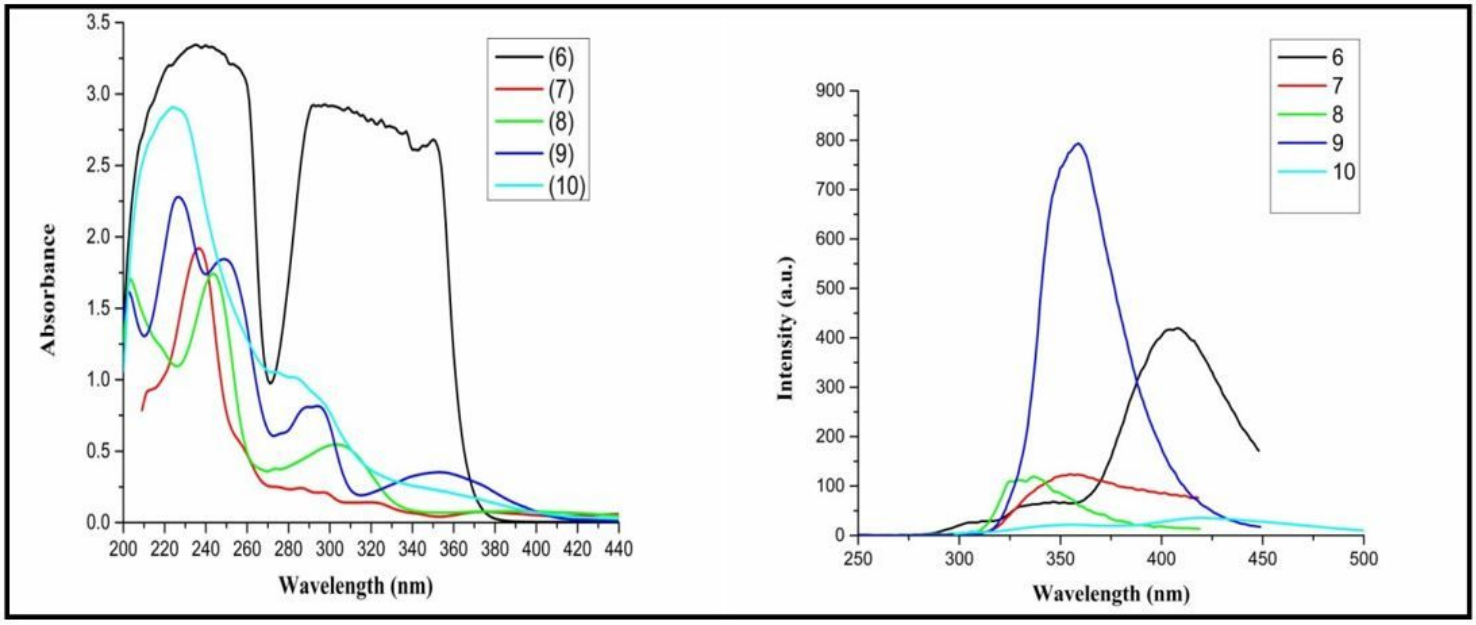

Figure 3

(a): UV-vis absorption spectra of compound (6-10) in DMSO solution. (b): Fluorescence emission spectra of the compound (6-10) at excitation wavelength of 280 nm in DMSO solution at RT.

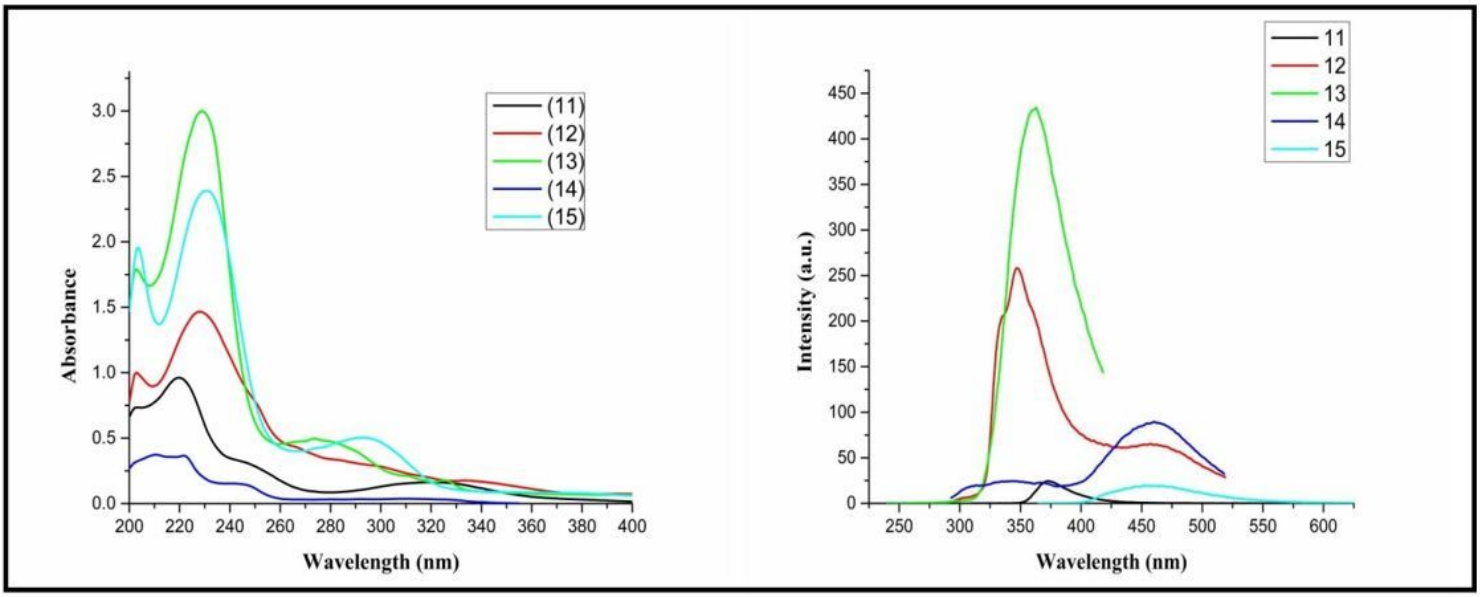

Figure 4

(a): UV-vis absorption spectra of compound (11-15) in DMSO solution. (b): Fluorescence emission spectra of the compound (11-15) at excitation wavelength of 280 nm in DMSO solution at RT.

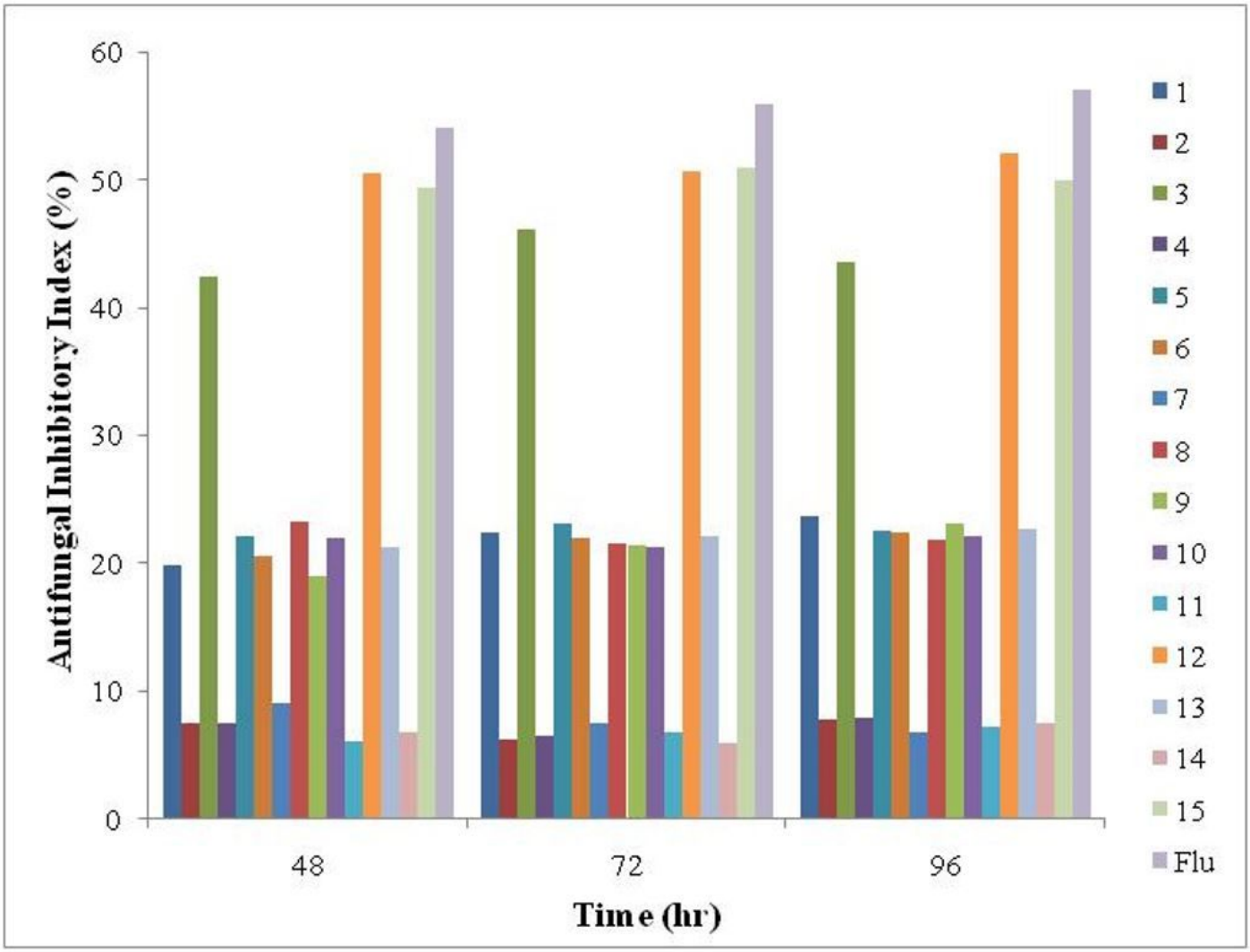

Figure 5

Antifungal inhibitory index for all the synthesized compounds against Aspergillus fumigates 3007 at different time intervals

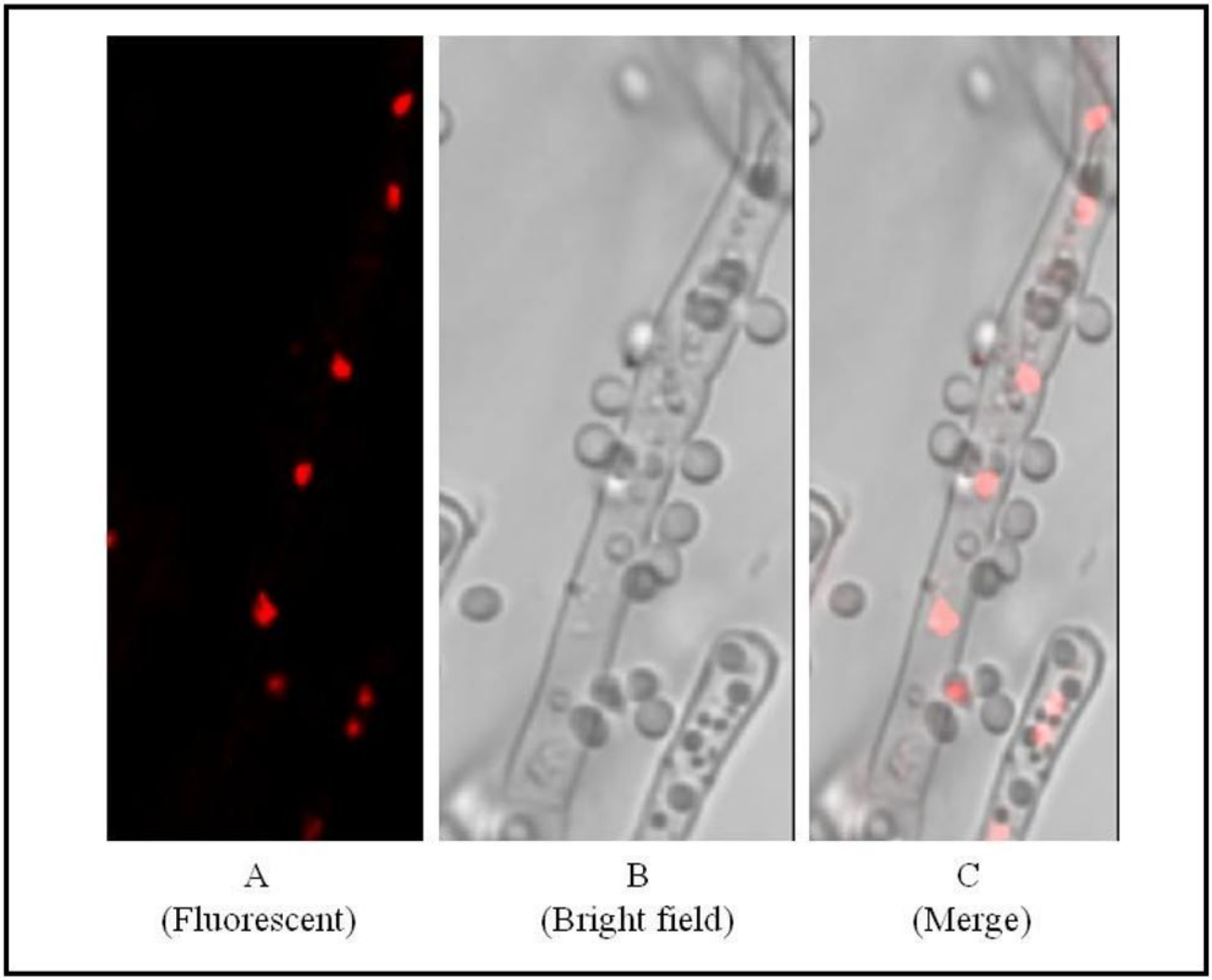

Figure 6

Confocal laser scanning microscope images of Aspergillus fumigatus 3007 depicting the effect of synthesized compound 12 on fungal membrane integrity.

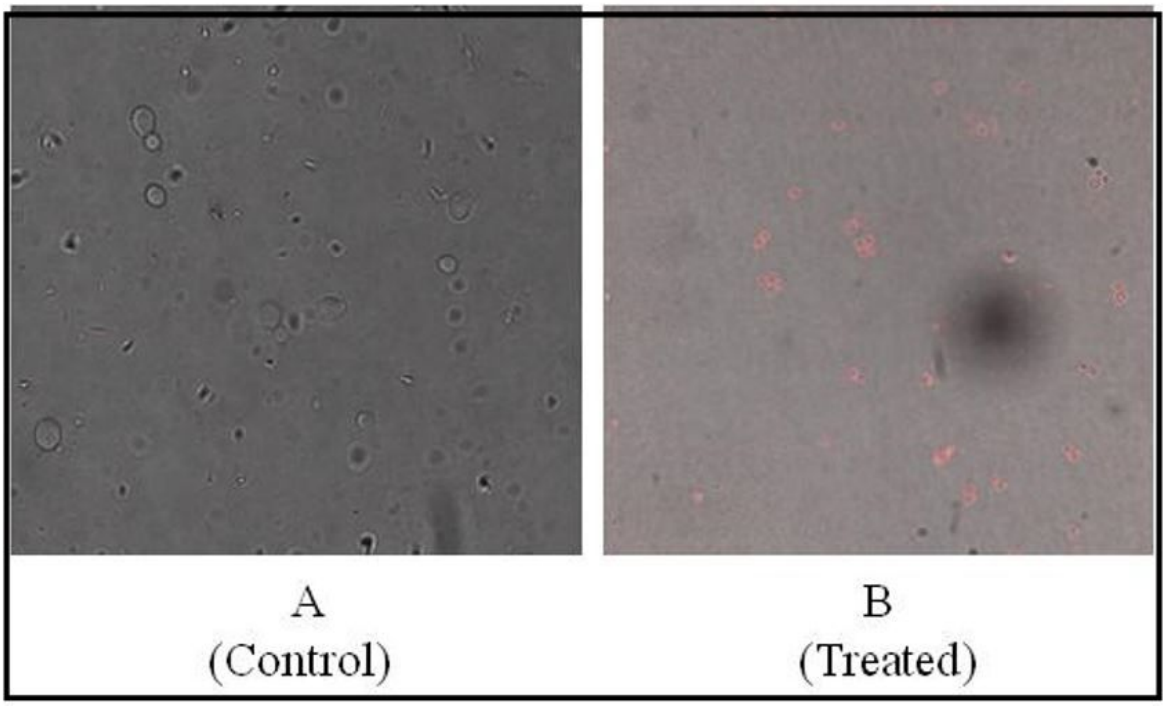

Figure 7

Confocal laser scanning microscope images of Candida albicans 3018 depicting the fluorescence from compound 12 treated samples

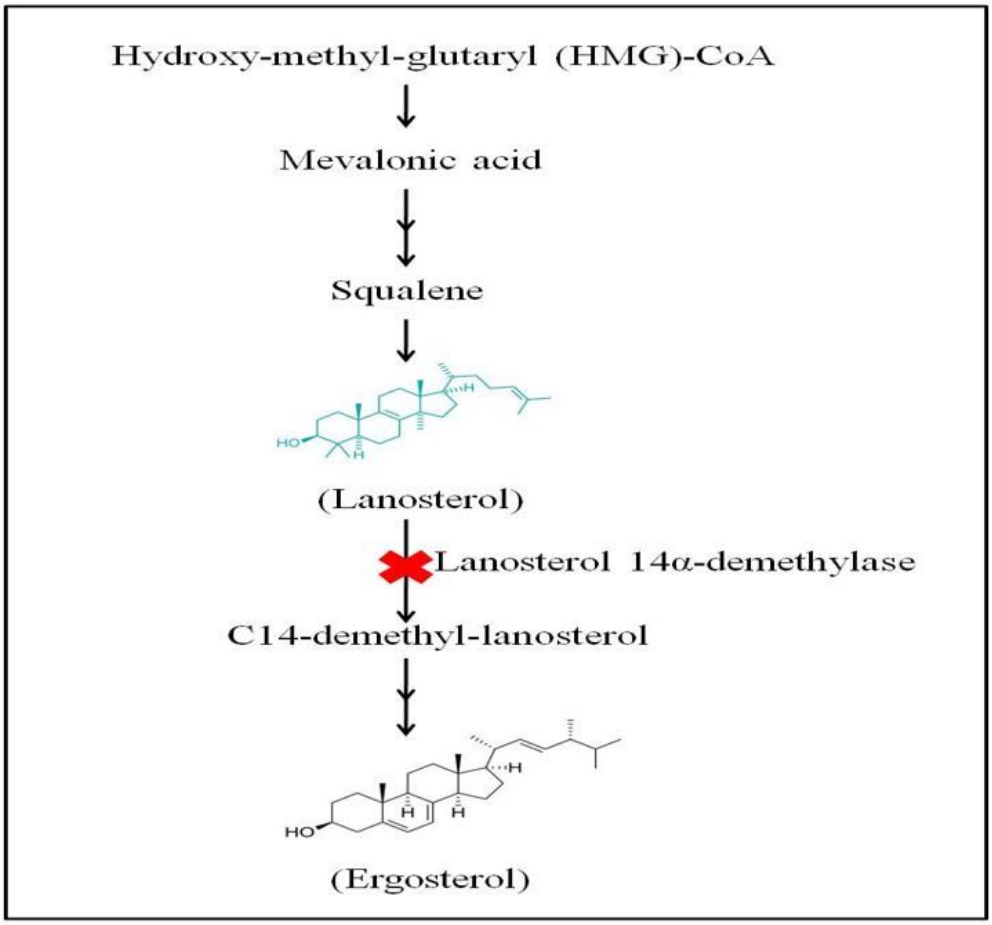

Figure 8

Ergosterol biosynthetic pathway

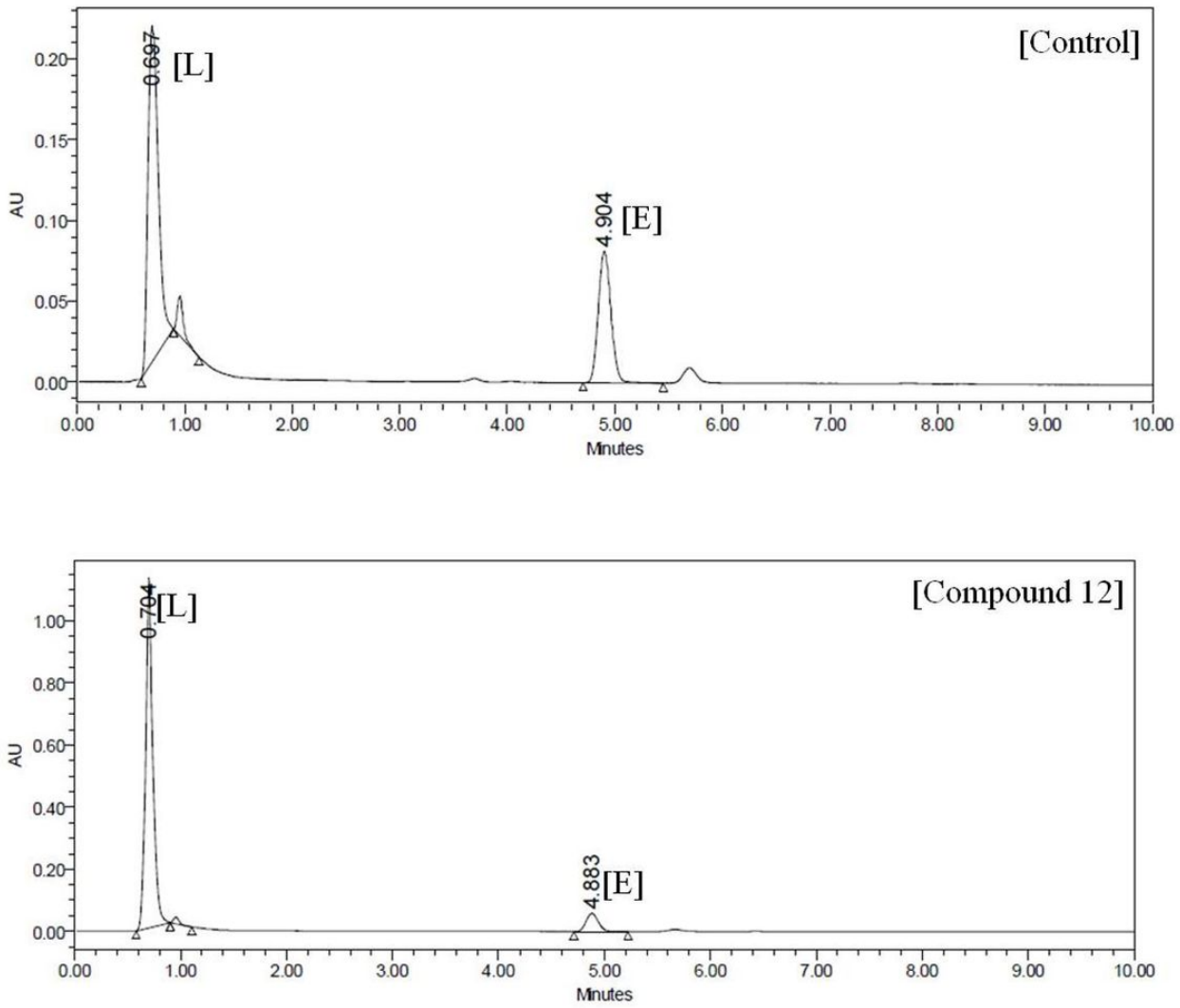

Figure 9

Ultrahigh-performance liquid chromatography chromatogram of extracted sterols ([L] peak for lanosterol and [E] peak for ergosterol)

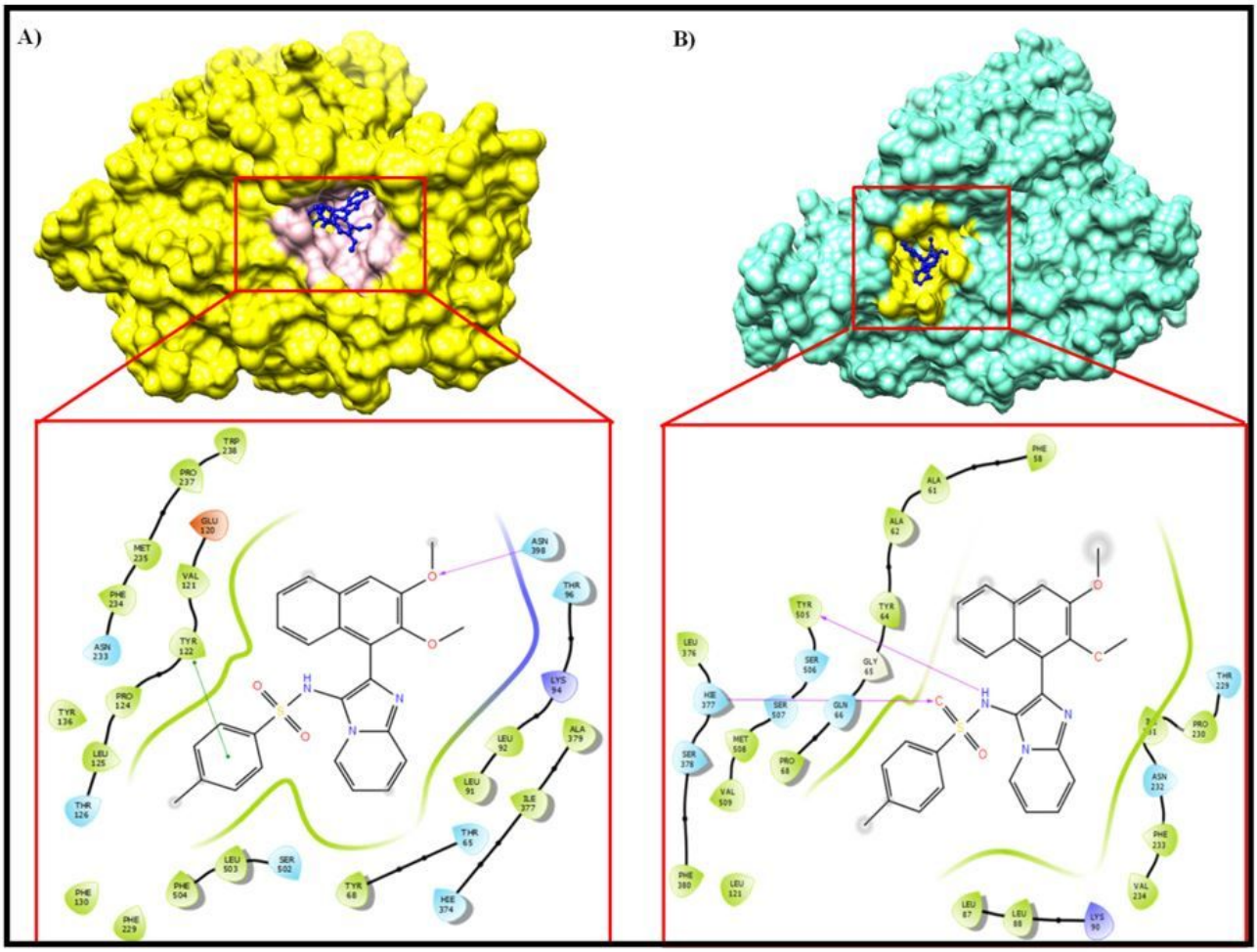

Figure 10

Surface representation of CYP51 from Aspergillus fumigatus (yellow; A) and Candida albicans (cyan; B) docked to compound 12 (blue ball and stick model) highlighting the protein-ligand interactions (within 5 Å) (square boxes).

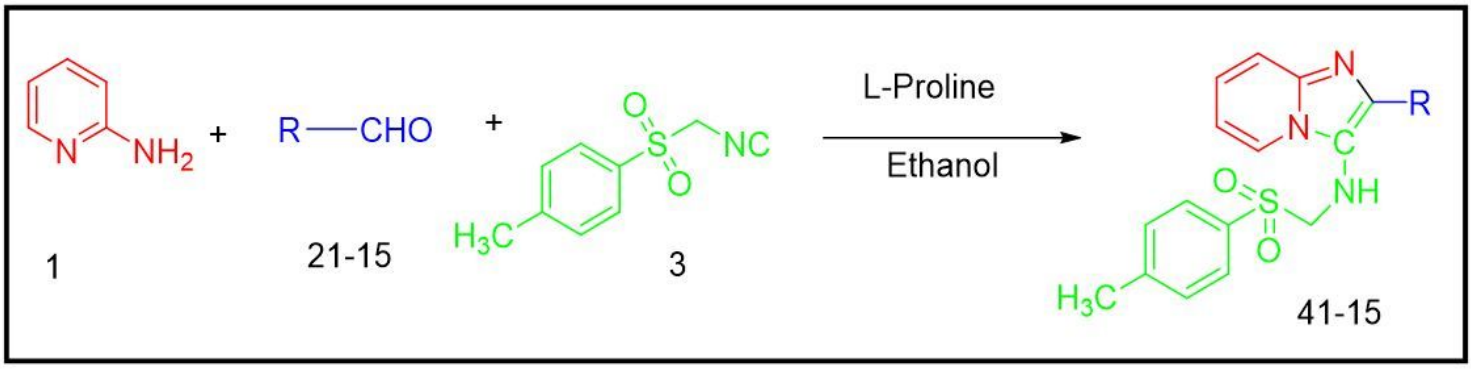

Figure 11

Model Reaction

Supplementary Files

This is a list of supplementary files associated with this preprint. Click to download.

- Supplementary.docx